



# CHORUS

This is the accepted manuscript made available via CHORUS. The article has been published as:

## Optimal-speed unitary quantum time evolutions and propagation of light with maximal degree of coherence

Carlo Cafaro, Shannon Ray, and Paul M. Alsing

Phys. Rev. A **105**, 052425 — Published 18 May 2022

DOI: [10.1103/PhysRevA.105.052425](https://doi.org/10.1103/PhysRevA.105.052425)

# Optimal-speed unitary quantum time evolutions and propagation of light with maximal degree of coherence

Carlo Cafaro<sup>1</sup>, Shannon Ray<sup>2</sup>, and Paul M. Alsing<sup>2</sup>

<sup>1</sup>*SUNY Polytechnic Institute, 12203 Albany, New York, USA and*

<sup>2</sup>*Air Force Research Laboratory, Information Directorate, 13441 Rome, New York, USA*

It is recognized that Grover arrived at his original quantum search algorithm inspired by his comprehension of the interference of classical waves originating from an array of antennae. It is also known that quantum-mechanical characterization of electromagnetic radiation is isomorphic to the treatment of the orientation of a spin-1/2 particle. In this paper, motivated by Grover's original intuition and starting from this mathematical equivalence, we present a quantitative link between the geometry of time-independent optimal-speed Hamiltonian evolutions on the Bloch sphere and the geometry of intensity-preserving propagation of light with maximal degree of coherence on the Poincaré sphere. Finally, identifying interference as the fundamental physical ingredient underlying both physical phenomena, we propose that our work can provide in retrospect a quantitative geometric background underlying Grover's powerful intuition.

PACS numbers: Quantum computation (03.67.Lx), Quantum information (03.67.Ac), Quantum mechanics (03.65.-w).

## I. INTRODUCTION

One of the main goals of quantum information science (QIS), including quantum nanoengineering and quantum optics, is the development of devices capable of reliably processing quantum information [1–3]. When considering the implementation of such quantum technologies, it becomes especially relevant engineering a suitable Hamiltonian that evolves an initial source state into a final target state. An essential condition for these quantum information processing devices is the capacity of having total control on the state of a single qubit on time scales much shorter than the coherence time. For such reasons, the conceptual understanding of controlled quantum dynamics along with their limits is becoming increasingly important in QIS. The cost functional that quantifies the efficiency of getting to the target state from a given initial state depends on the physical scenario being considered. In the simplest case, one can focus on an unconstrained Hamiltonian time-evolution, except for a bound on the energy resource. Then, regarding time-optimality as the cost functional, the problem becomes finding the time-independent Hamiltonian that generates maximum speed of evolution. However, there can be a range of constraints that forbids the implementation of such an elementary protocol in more realistic scenarios. Indeed, in real laboratory settings needed for the implementation of quantum technologies, one would need to apply various optimization techniques available within the more general framework of optimal quantum control theory [4] to identify suitable time-dependent Hamiltonians that generate the dynamics achieving required quantum tasks. The transition to time-dependent Hamiltonians can be motivated by several reasons, including the presence of time-varying external magnetic fields [5] or, alternatively, the existence of dissipation due to a coupling between the quantum system and the environment [6]. From this wide range of physical scenarios that one could take into consideration, we shall focus in this paper on the simplest case, namely that of time-optimal quantum mechanical unitary evolution in the presence of a bound on the energy resource.

It is known that the quantum-mechanical treatment of photon polarization is mathematically equivalent to the treatment of the orientation of a spin-1/2 particle [7]. In particular, focusing on the physics of two-level quantum systems and classical polarization optics in two-dimensions, the concepts of Bloch vector and Bloch sphere [8] are the analogues of the notions of Stokes vector and Poincaré sphere [9], respectively.

A remarkable link between quantum mechanics and classical optics is represented by the interpretation of Pancharatnam's optical phase that appears in the context of interference of polarized light [10] as an early example of Berry's (nondynamical) geometric phase that emerges in the context of cyclic and adiabatic quantum mechanical evolutions [11]. For an in-depth discussion on the relation between Pancharatnam's phase and Berry's phase, we refer to Refs. [12, 13]. The work in Ref. [12] is especially illuminating since Berry, starting from the description of polarization in terms of the Poincaré sphere, expresses Pancharatnam's classical optics analysis in quantum mechanical language and, moreover, clarifies the relation between the classical optical phase and the quantum adiabatic phase. Interestingly, this mutual interaction between quantum mechanics and classical optics has been rather beneficial in science. For example, borrowing ideas from Pancharatnam's work on the classical interference of polarized light, Samuel and Bhandari extended the concept of Berry's phase to nonunitary and noncyclic quantum mechanical evolutions in Ref. [13]. Furthermore, just as Pancharatnam's theory was tested in an experimental fashion with the detection of the predicted phase shifts by interference, the first experimental manifestation of Berry's phase was carried out in an op-

tical experiment [14] where the Berry phase measured corresponded to an angle of rotation of a plane of polarization of light [15]. A second close similarity between quantum mechanics and classical optics is the correspondence between the degree of polarization of beams of light and the parity of qubits as reported in Refs. [16, 17]. The origin of this similarity can be explained as follows. In the quantum mechanical Bloch sphere formalism, the origin represents a maximally mixed state, whereas points on the surface of the sphere are pure states. In the Poincaré sphere formalism in classical optics, the origin represents a completely unpolarized light beam, whereas points on the surface of the sphere are completely polarized beams.

In quantum mechanics, there are several ways in which one can derive an expression of time-independent optimal-speed Hamiltonians evolving an initial state  $|A\rangle$  into a final state  $|B\rangle$ . For instance, a simple derivation can rely on finding Hamiltonians  $\{H\}$  that evolve  $|A\rangle$  into  $|B\rangle$  in the least time subject to the constraint that the difference between the largest and the smallest eigenvalues of  $H$  is held fixed [18]. Another straightforward derivation, instead, can put the emphasis on choosing the Hamiltonian so that the uncertainty in energy is maximized [19]. In any case, the trajectories connecting  $|A\rangle$  and  $|B\rangle$  generated by such optimal-speed unitary evolutions  $\{U\}$  can be viewed as geodesic curves on the Bloch sphere (or, alternatively, the two-sphere  $S^2$ ). For this reason, it is especially interesting the geometric interpretation of these unitary operators  $\{U\}$  with  $|A\rangle \xrightarrow{U} |B\rangle$  in terms of rotations of the Bloch sphere around the axis that is orthogonal to the hemispherical plane containing the origin along with  $|A\rangle$  and  $|B\rangle$ . In particular, the Hamiltonian that generates the rotation takes the form  $H = E_+ |E_+\rangle \langle E_+| + E_- |E_-\rangle \langle E_-|$  for a pair of real parameters  $E_\pm$  with the axis of rotation corresponding to a pair of orthogonal states  $|E_\pm\rangle$  [20, 21]. More generally, given that the dynamics induced by a optimal-speed unitary evolution can be regarded as a rigid rotation of the two-sphere  $S^2$ , if there exists a unitary evolution transforming  $|A\rangle$  into  $|B\rangle$  with  $\langle A|B\rangle = 0$  along a geodesic path, then there must exist a pair of energy eigenstates  $|E_+\rangle$  and  $|E_-\rangle$ , say at the equator of  $S^2$ , such that  $|A\rangle$  and  $|B\rangle$  lie at the poles of  $S^2$  [22]. Moreover, in terms of an efficiency measure defined by means of the ratio between the distance along the shortest geodesic path joining  $|A\rangle$  and  $|B\rangle$  and the distance along the actual dynamical trajectory traced by the state vector  $|\psi(t)\rangle \stackrel{\text{def}}{=} e^{-\frac{i}{\hbar}Ht} |A\rangle$ , these optimal-speed unitary quantum mechanical evolutions exhibit unit “*quantum geometric efficiency*” [23, 24].

In classical polarization optics, it is known that the degree of polarization of a light wave propagating along the  $\hat{z}$ -direction does not depend on the choice of the  $\hat{x}$ - and  $\hat{y}$ -directions. Furthermore, such a degree of polarization is an upper bound for the so-called degree of coherence between the electric vibrations in the  $\hat{x}$ - and  $\hat{y}$ -directions [9]. Interestingly, it can be demonstrated that there always exists a pair of orthogonal directions for which the degree of coherence has its maximum value and this value is equal to the degree of polarization of the light wave [25]. Therefore, considering the ratio between the degree of coherence and the degree of polarization as some sort of “*classical optical efficiency*”, it happens that there is always an optimal optical configuration in which the propagation of polarized light occurs with maximal degree of coherence.

In this paper, we wish to investigate an unexplored link between optimal-speed quantum mechanical evolutions and propagation of light with maximal degree of coherence. Our investigation is inspired by the above mentioned existing links between quantum mechanics and classical optics. Furthermore, we rely on our familiarity with both digital and analog quantum search algorithms [24, 26–30]. In addition, our proposed investigation finds additional motivation by recalling that Grover’s original intuition that helped him creating his quantum search algorithm [31] was based upon a classical optics phenomenon. Specifically, Grover arrived at his quantum search algorithm by observing the interference of classical waves originating from an array of antennae [32]. This way, by mimicking the interference of *classical* waves, Grover arrived at his *quantum* search scheme.

Therefore, motivated by this intriguing similarity between the existence of a convenient pair of orthogonal energy eigenstates in the geometrical description of optimal-speed quantum evolutions and the existence of a suitable pair of orthogonal directions for the electric field in the geometric description of propagation of polarized light with optimal-coherence, we provide in this paper a quantitative link between quantum mechanics and classical polarization optics. Specifically, starting from the mathematical equivalence between the quantum-mechanical characterization of electromagnetic radiation and the treatment of the orientation of a spin-1/2 particle, we discuss in a quantitative manner the connection between the geometry of time-independent optimal-speed Hamiltonian evolutions on the Bloch sphere and the geometry of intensity-preserving propagation of light with maximal degree of coherence on the Poincaré sphere. Identifying interference as the essential physical ingredient underlying both phenomena being studied in our paper, we conclude by arguing that our work can provide a quantitative geometric background underlying Grover’s powerful intuition.

**To summarize, we are aware of the following known links: i) Connection between interference in classical wave theory and interference in quantum mechanics; ii) Equivalence between the Bloch sphere and the Poincaré sphere. In this paper, however:**

- We provide a novel and unnoticed link between *the geometry of the unitary dynamics of time-independent optimal-speed Hamiltonians on the Bloch sphere and the geometry of intensity-*

***preserving propagation of light with maximal degree of coherence on the Poincaré sphere. Our finding establishes a new bridge between the physics of two-level quantum systems and the physics of classical polarization optics via the discovery of this previously unknown connection.***

The layout of the remainder of this paper is as follows. In Section II, we discuss two alternative characterizations of optimal-speed Hamiltonians. The first analysis focuses on minimizing the evolution time subject to the energy eigenvalue constraint. The second one, instead, relies on the maximization of the energy uncertainty that yields the spectral decomposition of the optimal Hamiltonian. We conclude Section II with a discussion on unit geometric efficiency on the Bloch sphere. In Section III, after providing some motivational background, we characterize the propagation of light in terms of the polarization ellipse, the Stokes parameters, and the Poincaré sphere. Then, we briefly present the concepts of coherence of electric vibrations along with degree of coherence, coherency matrix, and degree of polarization of a light wave. In Section IV, we discuss the propagation of polarized light with maximal degree of coherence, that is propagation of light with unit optical efficiency on the Poincaré sphere. The quantitative link between the geometry of time-independent optimal-speed Hamiltonian evolutions on the Bloch sphere and the geometry of intensity-preserving propagation of light with maximal degree of coherence on the Poincaré sphere is carried out throughout Sections II and IV. In Section V, we discuss the physical origin of our proposed link. Our concluding remarks appear in Section VI. A number of technical details and remarks appear in Appendices A, B, C, and D. Specifically, in Appendix A we place some specific properties of the Mueller matrices in optics. In this Appendix B, we employ the Poincaré sphere formalism to describe the dependence of the modulus of the complex degree of coherence of a partially polarized light beam in terms of the ellipticity and orientation angles. In this Appendix C, we report some mathematical details on the parametrization of qubits and polarization states regarded as points on the Bloch sphere and the Poincaré sphere, respectively. Finally, we present in Appendix D a discussion on the role played by interference effects in light propagation, quantum searching, and optimal-speed quantum evolutions.

## II. QUANTUM EVOLUTIONS WITH UNIT GEOMETRIC EFFICIENCY

In this section, we discuss two alternative descriptions of optimal-speed Hamiltonians. The first characterization focuses on minimizing the evolution time subject to the energy eigenvalue constraint. The second one, instead, depends on the maximization of the energy uncertainty that leads to the spectral decomposition of the optimal Hamiltonian. We conclude this section with a discussion on unit geometric efficiency on the Bloch sphere.

When studying the geometric characterization of unit efficiency [23] quantum mechanical unitary evolutions specified by time-independent Hamiltonians  $\{H\}$  under which a normalized initial state vector  $|A\rangle$  evolves into a normalized final state vector  $|B\rangle$ , one notices at least two alternative approaches in the literature. In a first approach, researchers aim to find an expression of the Hamiltonian by minimizing the evolution time  $\Delta t \stackrel{\text{def}}{=} T_{AB}$  needed for evolving  $|A\rangle$  into  $|B\rangle$  subject to the constraint that the difference between the largest ( $E_+$ ) and smallest ( $E_-$ ) eigenvalues of the Hamiltonian is kept fixed [18],  $E_+ - E_- \stackrel{\text{def}}{=} E_0 = \text{fixed}$ . In a second approach, instead, investigators seek for an expression of the Hamiltonian by maximizing the uncertainty in energy  $\Delta E$  of the system [19]. This approach is motivated by the fact that the (angular) speed of the minimal-time evolution  $v$  of the quantum system is proportional to  $\Delta E$ ,  $v \stackrel{\text{def}}{=} ds_{\text{FS}}/dt \propto \Delta E$ , with  $s_{\text{FS}}$  denoting the Fubini-Study distance between the two points on the projective Hilbert space  $\mathcal{P}(\mathcal{H})$  that corresponds to the selected initial and final states  $|A\rangle$  and  $|B\rangle$ , respectively. Despite the fact that these two quantum approaches are essentially equivalent since the constraint on the difference between the largest and the smallest eigenvalues of the Hamiltonian is similar to upper bounding the energy uncertainty  $\Delta E$  since  $\Delta E_{\text{max}} = (E_+ - E_-)/2$ , they do put the emphasis on distinct features that will help us better understanding the details of the optimal evolution Hamiltonian. Ultimately, these complementary features will help us describing the formal analogies between the geometry of quantum evolutions with unit quantum geometric efficiency and the geometry of classical polarization optics for light waves with degree of polarization  $P$  that equals the degree of coherence  $|j_{xy}|$  between the electric vibrations in any two mutually orthogonal directions of propagation of the wave [25]. Unit quantum geometric efficiency means here that  $\eta_{\text{QM}} \stackrel{\text{def}}{=} s_0/s = 1$ , where  $s_0$  is the distance along the shortest geodesic joining the initial and final points of the evolution that are distinct on the projective Hilbert space while  $s$  is the distance along the effective evolution of the system in the projective Hilbert space as measured by the Fubini-Study metric. Finally, unit classical optical efficiency means here  $\eta_{\text{optics}} \stackrel{\text{def}}{=} |j_{xy}|/P = 1$ .

### A. Minimizing the evolution time

The starting point of the first approach can be summarized as follows. Given a time-independent Hamiltonian  $H$  with a corresponding unitary time-evolution operator  $U(t) \stackrel{\text{def}}{=} e^{-\frac{i}{\hbar}Ht}$ , one wishes to evolve a state  $|A\rangle$  into a state  $|B\rangle$  in the shortest possible time subject to the constraint that the difference  $E_+ - E_-$  between the largest ( $E_+$ ) and the smallest ( $E_-$ ) eigenvalues of  $H$  is kept fixed. In summary, we wish to find the optimal Hamiltonian acting in the two-dimensional subspace spanned by  $|A\rangle$  and  $|B\rangle$  that yields the optimal time evolution subject to the constraint  $E_+ - E_- \stackrel{\text{def}}{=} E_0$  is fixed.

We begin by considering the following unitary evolution scheme,

$$|A\rangle = \begin{pmatrix} \alpha_1 \\ \alpha_2 \end{pmatrix} \xrightarrow{e^{-\frac{i}{\hbar}Ht}} |B\rangle = \begin{pmatrix} \beta_1 \\ \beta_2 \end{pmatrix}, \text{ with } H \stackrel{\text{def}}{=} \begin{pmatrix} h_{11} & h_{12}e^{-i\phi} \\ h_{12}e^{i\phi} & h_{22} \end{pmatrix} \quad (1)$$

and, where  $h_{11}$ ,  $h_{12}$ ,  $h_{22}$ , and  $\phi$  are four real quantities. We assume that  $|A\rangle$  and  $|B\rangle$  are normalized to one so that  $|\alpha_1|^2 + |\alpha_2|^2 = 1$  and  $|\beta_1|^2 + |\beta_2|^2 = 1$ . The spectral decomposition of  $H$  in Eq. (1) can be recast as  $H = E_+ |E_+\rangle \langle E_+| + E_- |E_-\rangle \langle E_-|$  with the energy eigenvalue constraint given by,

$$(E_+ - E_-)^2 = (h_{11} - h_{22})^2 + 4h_{12}^2 = \text{constant} \stackrel{\text{def}}{=} E_0^2. \quad (2)$$

In view of our interest in studying the action of  $e^{-\frac{i}{\hbar}Ht}$  onto  $|A\rangle$ , it is convenient to observe that  $H$  in Eq. (1) can be decomposed in terms of the Pauli matrices  $\vec{\sigma} \stackrel{\text{def}}{=} (\sigma_x, \sigma_y, \sigma_z)$  as

$$H = \frac{h_{11} + h_{22}}{2} I + \frac{E_0}{2} \hat{a} \cdot \vec{\sigma}. \quad (3)$$

In Eq. (3),  $I$  denotes the identity matrix while  $\hat{a} \stackrel{\text{def}}{=} \vec{a} / \|\vec{a}\|$  with  $\|\vec{a}\| = E_0/2$  is a unit vector defined as,

$$\hat{a} \stackrel{\text{def}}{=} \frac{2}{E_0} \left( h_{12} \cos(\phi), h_{12} \sin(\phi), \frac{h_{11} - h_{22}}{2} \right). \quad (4)$$

We emphasize at this stage that finding the optimal evolution Hamiltonian reduces to finding the optimal set of the four real parameters  $\{h_{11}, h_{12}, h_{22}, \phi\}$  in Eq. (1) or, equivalently, the optimal  $\hat{a}$  that appears in Eq. (3). Using Eq. (3) along with algebraic manipulations that are typical in quantum mechanics with Pauli matrices, the action of  $e^{-\frac{i}{\hbar}Ht}$  onto  $|A\rangle$  leading to the state  $|B\rangle$  in a time  $T_{AB}$  yields

$$\begin{pmatrix} \beta_1 \\ \beta_2 \end{pmatrix} = e^{-\frac{i}{\hbar} \frac{h_{11} + h_{22}}{2} T_{AB}} \left( \alpha_1 \begin{bmatrix} \cos\left(\frac{E_0}{2\hbar} T_{AB}\right) - i \frac{h_{11} - h_{22}}{E_0} \sin\left(\frac{E_0}{2\hbar} T_{AB}\right) \\ \alpha_1 \left[ -ie^{i\phi} \frac{2h_{12}}{E_0} \sin\left(\frac{E_0}{2\hbar} T_{AB}\right) \right] \end{bmatrix} + \alpha_2 \begin{bmatrix} -ie^{-i\phi} \frac{2h_{12}}{E_0} \sin\left(\frac{E_0}{2\hbar} T_{AB}\right) \\ \cos\left(\frac{E_0}{2\hbar} T_{AB}\right) + i \frac{h_{11} - h_{22}}{E_0} \sin\left(\frac{E_0}{2\hbar} T_{AB}\right) \end{bmatrix} \right). \quad (5)$$

At this point, we note that the components of the states  $|A\rangle$  and  $|B\rangle$  depend on the choice of the basis of the two-dimensional subspace spanned by these two vectors. Therefore, for the sake of computational simplicity and without loss of generality, we choose a basis so that  $|A\rangle = (1, 0)$  and  $|B\rangle = (\alpha, \beta)$ . With this choice, Eq. (5) reduces to

$$\begin{pmatrix} \alpha \\ \beta \end{pmatrix} = e^{-\frac{i}{\hbar} \frac{h_{11} + h_{22}}{2} T_{AB}} \begin{pmatrix} \cos\left(\frac{E_0}{2\hbar} T_{AB}\right) - i \frac{h_{11} - h_{22}}{E_0} \sin\left(\frac{E_0}{2\hbar} T_{AB}\right) \\ -ie^{i\phi} \frac{2h_{12}}{E_0} \sin\left(\frac{E_0}{2\hbar} T_{AB}\right) \end{pmatrix}. \quad (6)$$

Considering the modulus of  $\beta$  as expressed in Eq. (6), we note that the expression of the evolution time  $T_{AB}$  becomes

$$T_{AB} = \frac{2\hbar}{E_0} \sin^{-1} \left( \frac{E_0 |\beta|}{2h_{12}} \right). \quad (7)$$

We observe that the  $\sin^{-1}(x)$  function is a monotonic increasing function of its argument  $x$  with  $\sin^{-1}(0) = 0$ . Therefore, since  $E_0$  and  $|\beta|$  are held fixed, the minimum value of  $T_{AB}$  in Eq. (7) is reached when  $h_{12}$  assumes its maximum possible value. The maximum possible value  $h_{12}^{\text{max}}$  of  $h_{12}$  compatible with the eigenvalue constraint in Eq. (2) is reached when  $h_{11} = h_{22}$  and equals  $h_{12}^{\text{max}} = E_0/2$ . Therefore, the optimal evolution time  $T_{AB}^{\text{min}} = T_{AB}(h_{12}^{\text{max}})$  is equal to

$$T_{AB}^{\text{min}} = \frac{2\hbar}{E_0} \sin^{-1}(|\beta|), \quad (8)$$

or, equivalently,  $T_{AB}^{\min} = (2\hbar/E_0) \cos^{-1}(|\alpha|)$  using the normalization condition  $|\alpha|^2 + |\beta|^2 = 1$  along with properties of the  $\sin^{-1}(x)$  function. So far, we have realized that the optimal set of the four real parameters  $\{h_{11}, h_{12}, h_{22}, \phi\}$  is specified by  $h_{12}^{\max} = E_0/2$  and  $h_{11} = h_{22}$ . Therefore, it remains to find the explicit expressions for the optimal  $h_{11}$  and  $\phi$ . These expressions can be found as follows. Let us set  $\alpha \stackrel{\text{def}}{=} |\alpha| e^{i\varphi_\alpha}$  and  $\beta \stackrel{\text{def}}{=} |\beta| e^{i\varphi_\beta}$  with  $\varphi_\alpha$  and  $\varphi_\beta$  in  $\mathbb{R}$ . Inserting Eq. (8) into Eq. (6), we obtain

$$\begin{pmatrix} |\alpha| e^{i\varphi_\alpha} \\ |\beta| e^{i\varphi_\beta} \end{pmatrix} = e^{-\frac{i}{\hbar} h_{11} T_{AB}^{\min}} \begin{pmatrix} \sqrt{1 - |\beta|^2} \\ -ie^{i\phi} |\beta| \end{pmatrix}. \quad (9)$$

With the help of some algebra, Eq. (9) yields

$$h_{11} = -\frac{\omega_0}{2} \frac{\varphi_\alpha}{\sin^{-1}(|\beta|)}, \text{ and } \phi = \varphi_\beta - \varphi_\alpha + \frac{\pi}{2}. \quad (10)$$

In conclusion, recalling the  $h_{12}^{\max} = E_0/2$  and  $h_{11} = h_{22}$  together with Eq. (10), the optimal evolution Hamiltonian can be recast as [33]

$$H = \frac{E_0}{2} \begin{pmatrix} \frac{\varphi_\alpha}{\sin^{-1}(|\beta|)} & e^{-i(\varphi_\beta - \varphi_\alpha - \frac{\pi}{2})} \\ e^{i(\varphi_\beta - \varphi_\alpha - \frac{\pi}{2})} & \frac{\varphi_\alpha}{\sin^{-1}(|\beta|)} \end{pmatrix}. \quad (11)$$

Interestingly, we note that the expectation value of the Hamiltonian  $\langle A|H|A \rangle$  is equal to  $(\varphi_\alpha E_0)/2 \sin^{-1}(|\beta|)$  while the energy uncertainty of H in Eq. (11) is given by  $\Delta E \stackrel{\text{def}}{=} \left[ \langle A|H^2|A \rangle - \langle A|H|A \rangle^2 \right]^{1/2} = E_0/2$ . Using the energy eigenvalue constraint in Eq. (2), we also notice that  $\Delta E = (E_+ - E_-)/2$ . As a final remark, we point out that since overall phases of state vectors have unobservable effects in quantum mechanics, the Hamiltonians H and  $H - (1/2)\text{tr}(H)I$  assume an identical maximal value  $\Delta E_{\max}$  of energy uncertainty  $\Delta E$ . Therefore, despite having different expectation values, these Hamiltonians generate the same physics of quantum evolutions. For this reason, for example, one may set the phase  $\varphi_\alpha$  in Eq.(11) equal to zero.

Starting from a traceless Hamiltonian with  $\Delta E_{\max} = (E_+ - E_-)/2$  will be the starting point in the second approach to optimal quantum evolutions that we treat in our paper. This second approach is based upon maximizing the energy uncertainty rather than minimizing the time evolution and will be discussed in the next subsection.

## B. Maximizing the energy uncertainty

The starting point of the second approach can be summarized as follows. Consider a time-independent and traceless Hamiltonian H with a spectral decomposition given by  $H = E_- |E_- \rangle \langle E_-| + E_+ |E_+ \rangle \langle E_+|$ , where  $E_+ \geq E_-$  and  $\langle E_+ | E_- \rangle = \delta_{+, -}$ . One wishes to evolve a state (not necessarily normalized)  $|A \rangle$  into a state  $|B \rangle$  in the shortest possible time by maximizing the energy uncertainty  $\Delta E \stackrel{\text{def}}{=} \left[ \langle A|H^2|A \rangle / \langle A|A \rangle - (\langle A|H|A \rangle / \langle A|A \rangle)^2 \right]^{1/2}$  and obtain  $\Delta E = \Delta E_{\max}$ .

For the sake of simplicity, we denote  $|E_\pm \rangle = |E_{2,1} \rangle$  and  $E_\pm = E_{2,1}$  in what follows. To find the value of  $\Delta E_{\max}$ , we note that an arbitrary unnormalized initial state  $|A \rangle$  can be decomposed as  $|A \rangle = \alpha_1 |E_1 \rangle + \alpha_2 |E_2 \rangle$  with  $\alpha_1, \alpha_2 \in \mathbb{C}$ . Then, after some algebra, we get

$$\Delta E = \frac{E_2 - E_1}{2} \left[ 1 - \left( \frac{|\alpha_1|^2 - |\alpha_2|^2}{|\alpha_1|^2 + |\alpha_2|^2} \right)^2 \right]^{1/2}. \quad (12)$$

From Eq. (12), we note that the maximum value of  $\Delta E$  is obtained for  $|\alpha_1| = |\alpha_2|$  (with  $\alpha_1$  and  $\alpha_2$  given by  $\langle E_1|A \rangle$  and  $\langle E_2|A \rangle$ , respectively) and equals  $\Delta E_{\max} \stackrel{\text{def}}{=} (E_2 - E_1)/2$  as mentioned in the previous subsection. The main underlying idea in this second approach is that of recasting  $H = E_1 |E_1 \rangle \langle E_1| + E_2 |E_2 \rangle \langle E_2|$  in terms of the initial and final states  $|A \rangle$  and  $|B \rangle$  while keeping,

$$\Delta E = \Delta E_{\max} \stackrel{\text{def}}{=} \frac{E_2 - E_1}{2}. \quad (13)$$

Observe that in terms of the eigenvectors of the Hamiltonian,  $|A\rangle$  and  $|B\rangle$  can be decomposed as  $|A\rangle = \alpha_1 |E_1\rangle + \alpha_2 |E_2\rangle$ , and  $|B\rangle = \beta_1 |E_1\rangle + \beta_2 |E_2\rangle$ , respectively. To ensure minimum travel time  $T_{AB}^{\min}$  (that is,  $\Delta E = \Delta E_{\max}$ ), we need to set  $|\alpha_1| = |\alpha_2|$  and  $|\beta_1| = |\beta_2|$ . Therefore, let  $\alpha_2 = e^{i\varphi_\alpha} \alpha_1$  and  $\beta_2 = e^{i\varphi_\beta} \beta_1$  with  $\varphi_{\alpha,\beta} \in \mathbb{R}$ . Then,  $|A\rangle$  and  $|B\rangle$  become

$$|A\rangle = \alpha_1 |E_1\rangle + \alpha_2 |E_2\rangle = \alpha_1 |E_1\rangle + e^{i\varphi_\alpha} \alpha_1 |E_2\rangle, \quad (14)$$

and,

$$|B\rangle = \beta_1 |E_1\rangle + \beta_2 |E_2\rangle = \beta_1 |E_1\rangle + e^{i\varphi_\beta} \beta_1 |E_2\rangle, \quad (15)$$

respectively. From Eqs. (14) and (15), we obtain  $|E_1\rangle + e^{i\varphi_\alpha} |E_2\rangle = \alpha_1^{-1} |A\rangle \stackrel{\text{def}}{=} \sqrt{2} |A\rangle$  and  $|E_1\rangle + e^{i\varphi_\beta} |E_2\rangle = \beta_1^{-1} |B\rangle \stackrel{\text{def}}{=} \sqrt{2} e^{-i\frac{\varphi_\alpha - \varphi_\beta}{2}} |B\rangle$ . After some matrix algebra, we get

$$\begin{pmatrix} |E_1\rangle \\ |E_2\rangle \end{pmatrix} = \frac{\sqrt{2}}{e^{i\frac{\varphi_\alpha + \varphi_\beta}{2}} - e^{i\varphi_\alpha} e^{i\frac{\varphi_\alpha - \varphi_\beta}{2}}} \begin{pmatrix} e^{i\frac{\varphi_\alpha + \varphi_\beta}{2}} & -e^{i\varphi_\alpha} \\ -e^{i\frac{\varphi_\alpha - \varphi_\beta}{2}} & 1 \end{pmatrix} \begin{pmatrix} \frac{\alpha_1^{-1}}{\sqrt{2}} |A\rangle \\ \frac{\beta_1^{-1}}{\sqrt{2}} e^{i\frac{\varphi_\alpha - \varphi_\beta}{2}} |B\rangle \end{pmatrix}. \quad (16)$$

For the sake of completeness, we emphasize that

$$|\langle \mathcal{A} | \mathcal{B} \rangle|^2 = \frac{|\langle A | B \rangle|^2}{\langle A | A \rangle \langle B | B \rangle} = \cos^2 \left( \frac{\varphi_\alpha - \varphi_\beta}{2} \right) = \cos^2 \left( \frac{\theta}{2} \right), \quad (17)$$

with  $\theta \stackrel{\text{def}}{=} \varphi_\alpha - \varphi_\beta = 2s_{\text{FS}} = s_{\text{geo}}$  where  $s_{\text{FS}}$  and  $s_{\text{geo}}$  denote the Fubini-Study and the geodesic distances, respectively. Finally, using Eq. (16) along with noting that  $E_2 = -E_1 \stackrel{\text{def}}{=} E$  since the Hamiltonian is assumed to be traceless, we obtain after some simple but tedious algebra that the spectral decomposition  $H = E_1 |E_1\rangle \langle E_1| + E_2 |E_2\rangle \langle E_2|$  becomes [34]

$$H = \frac{iE}{\sin \left( \frac{\varphi_\alpha - \varphi_\beta}{2} \right)} [|\mathcal{B}\rangle \langle \mathcal{A}| - |\mathcal{A}\rangle \langle \mathcal{B}|]. \quad (18)$$

In terms of the original initial and final states  $|A\rangle$  and  $|B\rangle$ , after some additional simple but laborious algebra, the Hamiltonian in Eq. (18) can be finally recast as

$$H = iE \cot \left( \frac{\varphi_\alpha - \varphi_\beta}{2} \right) \left[ \frac{|B\rangle \langle A|}{\langle A | B \rangle} - \frac{|A\rangle \langle B|}{\langle B | A \rangle} \right], \quad (19)$$

while the geodesic line  $|\psi(t)\rangle = e^{-\frac{i}{\hbar} H t} |A\rangle$  with  $H$  in Eq. (19) connecting the two states  $|A\rangle$  and  $|B\rangle$  can be written as

$$|\psi(t)\rangle = \left[ \cos \left( \frac{E}{\hbar} t \right) - \frac{\cos \left( \frac{\varphi_\alpha - \varphi_\beta}{2} \right)}{\sin \left( \frac{\varphi_\alpha - \varphi_\beta}{2} \right)} \sin \left( \frac{E}{\hbar} t \right) \right] |A\rangle + \frac{e^{i\frac{\varphi_\alpha - \varphi_\beta}{2}}}{\sin \left( \frac{\varphi_\alpha - \varphi_\beta}{2} \right)} \sin \left( \frac{E}{\hbar} t \right) |B\rangle, \quad (20)$$

where  $0 \leq t \leq T_{AB}^{\min}$  with  $T_{AB}^{\min} = \hbar\theta / (2E)$ . For the sake of completeness, we note that for  $H$  in Eq. (19), we correctly get  $\langle A | H | A \rangle / \langle A | A \rangle = 0$  and  $\Delta E = [\langle A | H^2 | A \rangle / \langle A | A \rangle]^{1/2} = E = \Delta E_{\max}$ . In conclusion, the Hamiltonians in Eqs. (11) and (19) are optimal-speed Hamiltonians yielding unit quantum geometric efficiency  $\eta_{\text{QM}} = 1$ . For clarity, we emphasize that Hamiltonians in Eqs. (11) and (19) are both optimal speed Hamiltonians. However, the Hamiltonian  $H$  in Eq. (11) is not traceless and its applicability is formally limited to connecting the initial state  $|A\rangle = (1, 0)$  to an arbitrary final state  $|B\rangle$ . The Hamiltonian  $H$  in Eq. (19), instead, is traceless and can connect an arbitrary initial state  $|A\rangle$  to an arbitrary final state  $|B\rangle$ .

Having discussed in detail the two main constructions of Hamiltonians yielding unit quantum geometric efficiency, in the next section we focus on the geometric characterization of the propagation of polarized light with maximal degree of coherence. As we present this classical optics description, we will emphasize analogies and determine exactly correspondences with the above mentioned quantum mechanical characterizations.

### III. PROPAGATION OF POLARIZED LIGHT AND DEGREE OF COHERENCE

In this section, we describe the propagation of light by means of the polarization ellipse, the Stokes parameters, and the Poincaré sphere. Then, we briefly define the notions of coherence of electric vibrations, degree of coherence, coherency matrix, and degree of polarization of a light wave. We end this section with a discussion on propagation of polarized light with maximal degree of coherence, that is, unit classical optical efficiency on the Poincaré sphere. However, before beginning with our formal descriptions, we present some motivational background that helps explaining our underlying motivations for presenting this material of polarization optics.

#### A. Motivational background

Two important quantities in optics when studying the physics of polarized light are the degree of polarization  $P$  of the wave and the degree of coherence  $|j_{xy}|$  of the electric vibrations. The quantity  $P$  is defined as [9],

$$P \stackrel{\text{def}}{=} \frac{I_{\text{pol}}}{I_{\text{tot}}}, \quad (21)$$

with  $I_{\text{tot}} \stackrel{\text{def}}{=} I_{\text{pol}} + I_{\text{unpol}}$  denoting the total intensity of the wave and  $I_{\text{pol}}$  being the intensity of the monochromatic (hence, polarized) part of the wave. The quantity  $P$  with  $0 \leq P \leq 1$  expresses the “amount of polarization” present in the wave. In particular, the wave is completely unpolarized when  $P = 0$  and completely polarized when  $P = 1$ . When  $0 < P < 1$ , the light is partially polarized. The degree of coherence  $|j_{xy}|$ , instead, is defined as the modulus of the complex degree of coherence  $j_{xy}$  [9],

$$j_{xy} \stackrel{\text{def}}{=} \frac{J_{xy}}{\sqrt{J_{xx}}\sqrt{J_{yy}}}. \quad (22)$$

In Eq. (22),  $J_{ij} \stackrel{\text{def}}{=} \langle E_i(t) E_j^*(t) \rangle$  are the matrix coefficients of the so-called coherency matrix  $J$  and the sharp brackets denote the time average operation. The quantity  $|j_{xy}|$  with  $0 \leq |j_{xy}| \leq |j_{xy}|_{\text{max}}$ , instead, measures the degree of correlation of the electric vibrations. When  $|j_{xy}| = 0$ , the electric vibrations are uncorrelated and they may be said to be incoherent. Furthermore, when  $|j_{xy}| = |j_{xy}|_{\text{max}}$ , the vibrations may be said to be coherent. Finally, when  $0 < |j_{xy}| < |j_{xy}|_{\text{max}}$ , vibrations are known as partially coherent. The quantity  $P$  can be fully expressed in terms of the determinant and the trace of the coherency matrix  $J$  as shown in Ref. [9]. Therefore, it is a quantity whose value does not change under arbitrary rotations of the orthogonal Cartesian axes used to describe the electric vibrations. However, unlike the degree of polarization of the wave, the degree of coherence  $|j_{xy}|$  between the electric vibrations in any two mutually orthogonal directions of propagation of the wave is generally affected by the specific choice of the two orthogonal directions [9]. In particular, it is possible to show that there always exist a pair of orthogonal directions for which the degree of coherence  $|j_{xy}|$  of the electric vibrations reaches its maximum value  $|j_{xy}|_{\text{max}}$  and, in addition, this value equals the degree of polarization  $P$  of the wave [25]. Interestingly, this particular pair of orthogonal directions has a clear geometrical interpretation. Indeed, representing the wave as an incoherent mixture of a wave of natural radiation and a wave of monochromatic (hence, completely polarized) radiation, it can be shown that these directions for which the degree of coherence  $|j_{xy}|$  equals the degree of polarization  $P$  are the bisectors of the principal directions (that is, major and minor axes) of the polarization ellipse of the polarized portion of the wave [35].

The existence of a pair of directions  $(\hat{x}', \hat{y}')$  rotated around the  $\hat{z}$ -axis (that is, the axis that specifies the direction of propagation of the wave) by a specific angle  $\varphi_{\text{opt}}$  that affects the electric vibrations in such a manner that the quantity  $\eta_{\text{opt}} \stackrel{\text{def}}{=} |j_{xy}|/P$ , that we name *classical optical efficiency* in this paper, equals one is reminiscent of the existence of a pair of orthogonal states  $(|E_+\rangle, |E_-\rangle)$  that defines the axis of rotation of the Bloch sphere orthogonal to the hemispherical plane containing the initial and final unit states  $|A\rangle$  and  $|B\rangle$  as discussed in the previous section. In the quantum case, this rotation around the  $\hat{n}_{E_+}$ -axis by an angle  $2 \cos^{-1} [|\langle A|B\rangle|]$  is essentially the unitary evolution operator emerging from the optimal-speed Hamiltonian that yields efficiency  $\eta_{\text{QM}} \stackrel{\text{def}}{=} s_0/s$  equal to one. Furthermore, just as these directions  $(\hat{x}', \hat{y}')$  for which  $|j_{xy}| = P$  are the bisectors of the principal directions  $(\hat{\xi}, \hat{\eta})$  corresponding to the major and minor axes, respectively, of the polarization ellipse, in a similar fashion, the pair of orthogonal states  $(|E_+\rangle, |E_-\rangle)$  for which  $s_0 = s$  lie in the equatorial plane when the pair of states  $(|A\rangle, |A_\perp\rangle)$  are assumed to lie at the poles. Finally, the angle  $\varphi_{\text{opt}}$  seems to be replaced in the quantum case by the azimuthal angle  $\varphi_{E_+}$  that serves to specify the location of  $|E_+\rangle$  on the Bloch sphere. We shall devote the rest of this paper to make these formal analogies as quantitative as possible. We shall begin by observing that to better characterize the propagation of the

Bloch Sphere	Polarization Ellipse	Poincaré Sphere
$( A\rangle,  A_\perp\rangle)$	$(\hat{\xi}, \hat{\eta})$	$\vec{S}_{\text{initial}}$
$( E_+\rangle_{\text{sub-optimal}},  E_-\rangle_{\text{sub-optimal}})$	$(\hat{x}, \hat{y})$	$\vec{S}_{\text{sub-optimal}}$
$( E_+\rangle_{\text{optimal}},  E_-\rangle_{\text{optimal}})$	$(\hat{x}', \hat{y}')$	$\vec{S}_{\text{optimal}}$
$\mathcal{H} = a_0 I + \vec{a} \cdot \vec{\sigma}$	$\vec{E}$	$J = \frac{1}{2} \vec{S} \cdot \vec{\sigma}$
$\hat{a} = \hat{a}(\theta, \varphi)$	$\vec{E} = \vec{E}(\beta, \chi)$	$\vec{S} = \vec{S}(2\beta, 2\chi)$
$e^{-i \frac{\ \vec{a}\  T_{AB}}{\hbar} \hat{a} \cdot \vec{\sigma}}$	$R_{\hat{z}}(\alpha)$	$M_{\text{ROT}}(\alpha)$
$s_0$ , fixed	$\vec{E}$ , fixed	$P$ , fixed
$s(0) \rightarrow s(T_{AB})$	$[\vec{E}]_{\{\hat{x}, \hat{y}\}} \rightarrow [\vec{E}]_{\{\hat{x}', \hat{y}'\}}$	$ j_{xy}  \rightarrow  j_{x'y'} $
$\eta_{\text{QM}} \stackrel{\text{def}}{=} s_0/s$	$\langle E_x E_x^* \rangle - \langle E_y E_y^* \rangle$	$\eta_{\text{optics}} \stackrel{\text{def}}{=}  j_{xy} /P$

TABLE I: Schematic depiction of the most relevant quantities that specify optimal-speed unitary quantum time evolutions on the Bloch sphere together with the analogue quantities that characterize the propagation of light with maximal degree of coherence by means of the polarization ellipse and the Poincaré sphere representations of polarized light.

effects of this simple two-dimensional rotation of the canonical Cartesian axes  $(\hat{x}, \hat{y})$  on the electric vibrations along with the coherency matrix  $J$  and, ultimately, on the degree of coherence  $|j_{xy}|$ , we need to better understand how to visualize and perform calculations when considering polarized light. For this reason, we shall introduce the concepts of polarization ellipse along with that of the Poincaré sphere.

To better motivate the definitions and concepts of polarization optics in what follows, we present in Table I a schematic depiction of the most relevant quantities that specify optimal-speed unitary quantum time evolutions on the Bloch sphere together with the analogue quantities that characterize the propagation of light with maximal degree of coherence by means of the polarization ellipse and the Poincaré sphere representations of polarized light. Clearly, these correspondences will become more transparent as we go through the next subsections and Section IV.

## B. Polarization of a light wave

In the previous section, we have explained how the Hamiltonian operator affects the path of evolution of a quantum system (specifically, a spin-1/2 particle) in terms of geometric evolutions on a Bloch sphere. In this section, keeping the directions of rays of light constant during its propagation, we focus on the state of polarization and the intensity of the light as it passes through an optical system. In this case, the three fundamental types of optical elements are wave plates, rotators, and polarizers. These elements give rise to phase shifting, rotations, and anisotropic attenuation, respectively. More specifically, we are interested here in intensity-preserving linear optical transformations which quantify the effect of rotators on polarized light in a geometric fashion. For such a quantification, we need to arrive at the Poincaré sphere description of polarized light. The way we plan to pursue this goal can be outlined as follows. Firstly, we begin with the polarization ellipse representation of polarized light [9]. Secondly, we introduce the Stokes parameters from the polarization ellipse [36]. Finally, we introduce the Poincaré sphere by attaching a geometric interpretation to the Stokes parameters [37]. We remark that the traditional language for studying the two-component electric vector of the light is the so-called Jones-matrix formalism based upon the use of  $2 \times 2$  complex matrices [38]. Alternatively, regarding the Stokes parameters as the components of a column matrix or 4-vector and optical devices as represented by  $4 \times 4$  matrices [39], the so-called Mueller matrix method can be employed to quantify the effect of optical devices on polarized light. For further details on the Mueller matrices in optics, we refer to Appendix A.

*Polarization ellipse.* Assume that the electric vector field  $\vec{E}$  of the light propagating along the  $\hat{z}$ -axis is given by  $\vec{E} = E_x(t)\hat{x} + E_y(t)\hat{y}$  with  $E_x(t)$  and  $E_y(t)$  defined as  $E_x(t) \stackrel{\text{def}}{=} E_{0x}(t) \cos[\omega t + \delta_x(t)]$  and  $E_y(t) \stackrel{\text{def}}{=} E_{0y}(t) \cos[\omega t + \delta_y(t)]$ , respectively. The quantities  $\omega$ ,  $\delta_x(t)$ , and  $\delta_y(t)$  specify the plane wave and denote the instantaneous angular frequency and the two instantaneous phases, respectively. After some algebraic manipulations of the two relations involving  $E_x(t)$  and  $E_y(t)$ , one arrives at an equation of an ellipse in a nonstandard form given by

$$\frac{E_x^2(t)}{E_{0x}^2(t)} + \frac{E_y^2(t)}{E_{0y}^2(t)} - \frac{2E_x(t)E_y(t)}{E_{0x}(t)E_{0y}(t)} \cos[\delta(t)] = \sin^2[\delta(t)], \quad (23)$$

with  $\delta \stackrel{\text{def}}{=} \delta_x - \delta_y$  [36]. The ellipse defined by Eq. (23) is not in its standard form since  $E_x(t)$  and  $E_y(t)$  are not directed along the  $\hat{x}$ - and  $\hat{y}$ -axes. Instead, they are directed along the  $\hat{\xi}$ - and  $\hat{\eta}$ -directions obtained from the canonical

Cartesian axes via a rotation around the  $\hat{z}$ -axis by an angle  $\chi$ . This angle is known as the orientation angle with  $0 \leq \chi < \pi$  and, clearly, it describes how tilted is the ellipse with respect to the canonical Cartesian axes. For the sake of completeness and later use, we also introduce at this point the so-called ellipticity angle  $\beta$  with  $-\pi/4 < \beta \leq \pi/4$  defined as  $\tan \beta \stackrel{\text{def}}{=} b/a$  with  $a$  and  $b$  being the major and minor axes of the polarization ellipse, respectively. This angle specifies the shape of the ellipse. In what follows, we introduce the Stokes parameters from the polarization ellipse.

*The Stokes parameters from the polarization ellipse.* Focusing on monochromatic radiation with  $E_{0x}$ ,  $E_{0y}$ ,  $\delta_x$ , and  $\delta_y$  constant in time, Eq. (23) reduces to

$$\frac{E_x^2(t)}{E_{0x}^2} + \frac{E_y^2(t)}{E_{0y}^2} - \frac{2E_x(t)E_y(t)}{E_{0x}E_{0y}} \cos \delta = \sin^2 \delta. \quad (24)$$

To represent Eq. (24) in terms of observables of the electromagnetic radiation, one needs to consider a time average over an infinite time interval. However, given the periodic behavior of  $E_x(t)$  and  $E_y(t)$ , averaging over a single period of vibration  $T$  will suffice. Specifically, define the time average of  $E_i(t)E_j(t)$  as

$$\langle E_i(t)E_j(t) \rangle \stackrel{\text{def}}{=} \frac{1}{T} \int_0^T E_i(t)E_j(t) dt. \quad (25)$$

Using Eq. (25), it can be shown following Ref. [36] that the time-averaged version of Eq. (24) can be recast as

$$S_0^2 = S_1^2 + S_2^2 + S_3^2, \quad (26)$$

with  $S_0 \stackrel{\text{def}}{=} E_{0x}^2 + E_{0y}^2$ ,  $S_1 \stackrel{\text{def}}{=} E_{0x}^2 - E_{0y}^2$ ,  $S_2 \stackrel{\text{def}}{=} 2E_{0x}E_{0y} \cos \delta$ , and  $S_3 \stackrel{\text{def}}{=} 2E_{0x}E_{0y} \sin \delta$ . The four parameters  $\{S_i\}$  with  $0 \leq i \leq 3$  are the observables of the polarization ellipse with  $S_0$  being the total intensity of the radiation while  $\{S_1, S_2, S_3\}$  specify the state of polarization of the light beam. These are the so-called four Stokes polarization parameters [40]. Eq. (26) holds for completely polarized light and  $S_0$  is redundant in this case. Instead, for partially polarized light,  $S_0^2 \geq S_1^2 + S_2^2 + S_3^2$  and  $S_0$  is no longer redundant. The excess  $S_0^2 - (S_1^2 + S_2^2 + S_3^2)$  indicates the amount of unpolarized light present in the beam. More specifically, for completely polarized light beams,  $S_0 \stackrel{\text{def}}{=} I_{\text{tot}} = I_{\text{pol}}$ . Instead, for partially polarized light,  $S_0 \stackrel{\text{def}}{=} I_{\text{tot}} > I_{\text{pol}}$ . We refer to Appendix B for details on the behavior of  $|j_{xy}|$  for partially polarized waves using the Poincaré sphere formalism.

In what follows, we introduce the Poincaré sphere by attaching a geometric interpretation to the Stokes parameters.

*The Poincaré sphere from the Stokes parameters.* It can be verified by a straightforward but tedious computation as mentioned in Refs. [37, 41] that for a fixed value of  $S_0$ , we have for completely polarized light  $S_1 \stackrel{\text{def}}{=} S_0 \cos(2\beta) \cos(2\chi)$ ,  $S_2 \stackrel{\text{def}}{=} S_0 \cos(2\beta) \sin(2\chi)$ , and  $S_3 \stackrel{\text{def}}{=} S_0 \sin(2\beta)$  with  $\beta$  and  $\chi$  being the ellipticity and orientation angles, respectively, as previously defined. Setting  $S_0 = 1$ , the quantities  $\{S_1, S_2, S_3\}$  have the following geometric interpretation. Consider the vector  $\vec{s} \stackrel{\text{def}}{=} (S_1, S_2, S_3)$  with length  $\|\vec{s}\| = S_0 = 1$ . The vector  $\vec{s}$  is located on a sphere of unit length with its location determined by the azimuth angle  $2\chi$  and the latitude angle  $2\beta$ . Thus, a beam of elliptically polarized light can be specified by the vector  $\vec{s}$  as mapped on the sphere as originally pointed out by Poincaré in Ref. [42]. For a graphical depiction of the Bloch and Poincaré spheres, we refer to Fig. 1. For more details on the parametrization of qubits and polarization states viewed as points on the Bloch sphere and the Poincaré sphere, respectively, we refer to Appendix C.

### C. Coherence of the electric vibrations

Having discussed the basics of polarized light, in this subsection we present the essentials concerning the notion of coherence of the electric vibrations.

Given the electric vector of the incident light wave in its complex form, the so-called coherency matrix  $J$  is defined as [25],

$$J = \begin{pmatrix} J_{xx} & J_{xy} \\ J_{yx} & J_{yy} \end{pmatrix} \stackrel{\text{def}}{=} \begin{pmatrix} \langle E_x E_x^* \rangle & \langle E_x E_y^* \rangle \\ \langle E_y E_x^* \rangle & \langle E_y E_y^* \rangle \end{pmatrix}, \quad (27)$$

where the sharp brackets denote time average. The coherency matrix  $J$  is an Hermitian matrix with  $J_{xy}^* = J_{yx}$  and characterizes the incident wave. In particular,  $\text{tr}(J)$  represents the intensity of the incident wave and its off-diagonal coefficients describe the correlation between the  $x$ - and  $y$ -components of  $\vec{E}$ . We observe that employing the

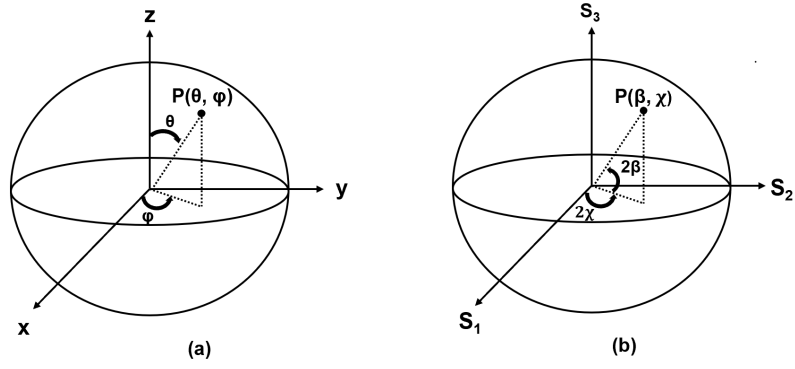


FIG. 1: In (a), we depict the Bloch sphere for pure quantum states of a single qubit. A point  $P = P(\theta, \varphi)$  on the surface of the Bloch sphere is defined by the Bloch vector  $\vec{r} \stackrel{\text{def}}{=} (r_x, r_y, r_z) = (r \sin \theta \cos \varphi, r \sin \theta \sin \varphi, r \cos \theta)$  with  $\|\vec{r}\| = 1$ . Mixed states are specified by  $\|\vec{r}\| \leq 1$ , with the origin representing a maximally mixed state. The angles  $\theta$  and  $\varphi$  are the polar and the azimuthal angles, respectively. In (b), we depict the Poincaré sphere of unit radius for the polarized state of a beam of light. A point  $P = P(\beta, \chi)$  on the surface of the Poincaré sphere is defined by the vector  $\vec{s} \stackrel{\text{def}}{=} (S_1, S_2, S_3) = (S_0 \cos 2\beta \cos 2\chi, S_0 \cos 2\beta \sin 2\chi, S_0 \sin 2\beta)$  where  $\vec{S} \stackrel{\text{def}}{=} (S_0, S_1, S_2, S_3)$  with  $S_1^2 + S_2^2 + S_3^2 = S_0^2 \equiv 1$  is the Stokes vector specified by the four Stokes parameters  $\{S_0, S_1, S_2, S_3\}$ . The parameter  $S_0$  denotes the total intensity of the beam while the remaining three parameters  $S_1, S_2$  and  $S_3$  specify the polarization state of the beam. A partially polarized beam of light is specified by  $S_0 \leq 1$ , with the origin being a completely unpolarized beam. Finally,  $\beta$  and  $\chi$  are the ellipticity and the orientation angles, respectively.

Schwarz inequality for integrals, it follows that  $|J_{xy}| \leq \sqrt{J_{xx}}\sqrt{J_{yy}}$  and  $|J_{yx}| \leq \sqrt{J_{yy}}\sqrt{J_{xx}}$ . Therefore,  $\det(J) \stackrel{\text{def}}{=} J_{xx}J_{yy} - J_{xy}J_{yx} \geq 0$ . The Stokes parameters can be expressed in terms of the coherency matrix coefficients by the relations  $S_0 \stackrel{\text{def}}{=} J_{xx} + J_{yy}$ ,  $S_1 \stackrel{\text{def}}{=} J_{xx} - J_{yy}$ ,  $S_2 \stackrel{\text{def}}{=} J_{xy} + J_{yx}$ , and  $S_3 \stackrel{\text{def}}{=} i(J_{yx} - J_{xy})$ . Inverting these equations, one gets  $J_{xx} = (S_0 + S_1)/2$ ,  $J_{yy} = (S_0 - S_1)/2$ ,  $J_{xy} = (S_2 + iS_3)/2$ , and  $J_{yx} = (S_2 - iS_3)/2$ . Therefore, the relation between the Stokes parameters  $\{S_0, S_1, S_2, S_3\}$  and the coherency matrix  $J$  can be recast in the following compact form [7, 25],

$$J = \frac{1}{2} \sum_{i=0}^3 S_i \sigma_i, \quad (28)$$

where in Eq. (28)  $\sigma_0 = I_{2 \times 2}$ ,  $\sigma_1 = \sigma_z$ ,  $\sigma_2 = \sigma_x$ ,  $\sigma_3 = -\sigma_y$  with  $\{\sigma_x, \sigma_y, \sigma_z\}$  being the usual Pauli spin matrices in quantum mechanics. To quantify the electric vibrations in the  $\hat{x}$ - and  $\hat{y}$ -directions, we introduce the so-called complex degree of coherence

$$j_{xy} = |j_{xy}| e^{i\beta_{xy}} \stackrel{\text{def}}{=} \frac{J_{xy}}{\sqrt{J_{xx}}\sqrt{J_{yy}}}. \quad (29)$$

In Eq. (29),  $|j_{xy}|$  is the modulus of the complex degree of coherence (we shall call it, degree of coherence) and measures the degree of correlation of the vibrations. The phase  $\beta_{xy} \in \mathbb{R}$ , instead, specifies the effective phase difference between the vibrations. As a side remark, we note that  $\det(J) \geq 0$  implies  $|j_{xy}| \leq 1$ . We notice that  $J$  in Eq. (27) will change if the  $\hat{x}$ - and  $\hat{y}$ -axes are rotated about the direction of propagation of the wave. Therefore, since  $|j_{xy}|$  is not expressed in terms of rotation-invariant terms, it depends on the choice of the  $\hat{x}$ - and  $\hat{y}$ -axes. Unlike  $|j_{xy}|$ , the degree of polarization  $P$  in Eq. (21) of a wave can be expressed in terms of rotation-invariant quantities built from the coherency matrix as we shall see in the next subsection.

#### D. Degree of polarization and coherency matrix

To express the degree of polarization of a wave in terms of the coherency matrix, we proceed as follows. Recall that a general coherency matrix  $J_{\text{general}}$  can be formally recast as,

$$J_{\text{general}} = \begin{pmatrix} J_{xx} & J_{xy} \\ J_{yx} & J_{yy} \end{pmatrix} \stackrel{\text{def}}{=} \begin{pmatrix} \alpha_1 & \gamma_1 - i\delta_1 \\ \gamma_1 + i\delta_1 & \beta_1 \end{pmatrix}, \quad (30)$$

Type of Sphere	Constraint Description	Constraint Equation
Bloch	bounded energy of the system	$(E_+ - E_-)^2 = (h_{11} - h_{22})^2 + 4h_{12}h_{21} = \text{fixed}$
Bloch	maximal energy dispersion	$\Delta E = \Delta E_{\text{max}}, \text{ and } \Delta t = \Delta t_{\text{min}}$
Poincaré	bounded intensity of light	$I_{\text{pol}}^2 = (J_{xx} - J_{yy})^2 + 4J_{xy}J_{yx} = \text{fixed}$
Poincaré	maximal correlations between $E_x$ and $E_y$	$S_2^2 = (S_2^2)_{\text{max}}, \text{ and } S_1^2 = 0$

TABLE II: Schematic summary of the main constraint equations yielding unit efficiency geodesic paths on the Bloch sphere and optical paths leading to polarization states with maximal degree of coherence on the Poincaré sphere.

with  $\alpha_1, \beta_1, \gamma_1, \delta_1 \in \mathbb{R}$ . Moreover, recall that any wave can be represented as a superposition of a wave of natural radiation with coherency matrix  $J_{\text{natural}} \stackrel{\text{def}}{=} [D^2, 0; 0, D^2]$  and a completely elliptically polarized (monochromatic) wave with coherency matrix  $J_{\text{pol}} \stackrel{\text{def}}{=} [A^2, -iAB; iAB, B^2]$  with  $A, B, D \in \mathbb{R}$ . Then, it can be shown that all light is a case or limiting case of partially elliptically polarized light with coherency matrix given by  $J_{\text{tot}} \stackrel{\text{def}}{=} J_{\text{natural}} + J_{\text{pol}}$ ,

$$J_{\text{tot}} = \begin{pmatrix} A^2 + D^2 & -iAB \\ iAB & B^2 + D^2 \end{pmatrix}. \quad (31)$$

To prove this statement, it is sufficient to show there exists a transformation that allows us to set Eq. (31) equal to Eq. (30). Indeed, it turns out that  $J_{\text{tot}} = T(\chi) \cdot J_{\text{general}} \cdot T^{-1}(\chi)$  where  $T(\chi) \stackrel{\text{def}}{=} [\cos \chi, \sin \chi; \sin \chi, -\cos \chi]$  is a real unitary transformation with  $\chi$  being the angle (that is, the orientation angle for the polarization ellipse that corresponds to the light beam) defined by the condition [43],

$$\tan(2\chi) = \frac{2\gamma_1}{\alpha_1 - \beta_1} = \frac{J_{xy} + J_{yx}}{J_{xx} - J_{yy}}. \quad (32)$$

For further details on how to express  $A, B,$  and  $D$  in terms of  $\alpha_1, \beta_1, \gamma_1, \delta_1$ , we refer to Ref. [43]. Now, setting  $J_{xx} \stackrel{\text{def}}{=} A^2 + D^2, J_{xy} \stackrel{\text{def}}{=} -iAB, J_{yx} \stackrel{\text{def}}{=} iAB,$  and  $J_{yy} \stackrel{\text{def}}{=} B^2 + D^2$ , we finally have

$$P \stackrel{\text{def}}{=} \frac{I_{\text{pol}}}{I_{\text{tot}}} = \frac{\text{tr}(J_{\text{pol}})}{\text{tr}(J_{\text{tot}})} = \left[ 1 - \frac{4 \det(J_{\text{tot}})}{[\text{tr}(J_{\text{tot}})]^2} \right]^{1/2}. \quad (33)$$

From Eq. (33), we note that  $P$  does not depend on the choice of the  $\hat{x}$ - and  $\hat{y}$ -directions. Furthermore, from Eq. (33) and the definition of  $|j_{xy}|$ , we obtain after some algebra that  $|j_{xy}| \leq P$  [25]. The equality  $|j_{xy}| = P$  holds iff  $J_{xx} = J_{yy}$ . It can be shown that a pair of orthogonal directions  $\hat{x}'$  and  $\hat{y}'$  always exist for which this is the case.

The fact that  $|j_{xy}|$  depends on the choice of the  $\hat{x}$  and  $\hat{y}$  directions while  $P$  does not, along with the definition of the angle  $\chi$  in Eq. (32), will play a major role in our discussion of unit optical efficiency in the next section.

#### IV. PROPAGATION OF LIGHT WITH UNIT OPTICAL EFFICIENCY

In this section, we finally describe the propagation of polarized light with maximal degree of coherence.

Let us define a measure of optical efficiency as the ratio between the degree of polarization of the wave and the degree of coherence of the electric vibrations,  $\eta_{\text{opt}} \stackrel{\text{def}}{=} |j_{xy}|/P$ . This quantity achieves its maximum value 1 when  $|j_{xy}| = P$ , that is to say, when  $J_{xx} = J_{yy}$ . For a fixed value of  $P$  or, analogously, for a fixed value of  $I_{\text{pol}} \stackrel{\text{def}}{=} \text{tr}(J_{\text{pol}}) = [(J_{xx} + J_{yy})^2 + 4 \det(J_{\text{pol}})]^{1/2} = \text{constant}$  [25], we wish to find a new pair of orthogonal directions  $\{\hat{x}', \hat{y}'\}$  such that  $J_{x'x'} = J_{y'y'}$  and, consequently,  $\eta_{\text{opt}} = 1$ . First, using the definition of  $\det(J_{\text{tot}})$ , we note that the constraint on  $I_{\text{pol}}$  can be recast as

$$I_{\text{pol}}^2 = (J_{xx} - J_{yy})^2 + 4J_{xy}J_{yx} = \text{constant}. \quad (34)$$

Therefore, from Eq. (34) we have that the optimal coherency matrix  $J'$  is specified by  $J_{x'x'} = J_{y'y'}$  and  $|J_{x'y'}| = I_{\text{pol}}/2$ . Observe that Eq. (34) is the analogue of Eq. (2). Furthermore, the quantum conditions  $h_{11} = h_{22}$  and  $h_{12}^{\text{max}} = E_0/2$  correspond to the optical conditions  $J_{x'x'} = J_{y'y'}$  and  $|J_{x'y'}| = I_{\text{pol}}/2$ , respectively.

Alternatively, in terms of the Stokes vector components, unit optical efficiency demands

$$S_1^2 \rightarrow (S_1^2)_{\min} = 0, \text{ with } S_2^2 \rightarrow (S_2^2)_{\max}. \quad (35)$$

Note that the minimization of  $S_1^2$  and the maximization of  $S_2^2$  correspond to the minimization of the evolution time and the maximization of the energy uncertainty, respectively. In Table II, we present a schematic of the main constraint equations yielding unit efficiency geodesic paths on the Bloch sphere (that is, Eqs. (2) and (13)) and optical paths leading to polarization states with maximal degree of coherence on the Poincaré sphere (that is, Eqs. (34) and (35)).

To find the pair of orthogonal directions  $\{\hat{x}', \hat{y}'\}$ , we assume they are obtained from the canonical Cartesian directions  $\{\hat{x}, \hat{y}\}$  via a rotation  $R_{\hat{z}}(\varphi_{\text{opt}}) \stackrel{\text{def}}{=} [\cos \varphi_{\text{opt}}, \sin \varphi_{\text{opt}}; -\sin \varphi_{\text{opt}}, \cos \varphi_{\text{opt}}]$  around the  $\hat{z}$ -axis by an angle  $\varphi_{\text{opt}}$  to be determined. Specifically, the components of the electric field  $\vec{E}$  with respect to the basis  $\{\hat{x}', \hat{y}'\}$  satisfy

$$\left[ \vec{E} \right]_{\{\hat{x}, \hat{y}\}} \rightarrow \left[ \vec{E} \right]_{\{\hat{x}', \hat{y}'\}} \stackrel{\text{def}}{=} R_{\hat{z}}(\varphi_{\text{opt}}) \cdot \left[ \vec{E} \right]_{\{\hat{x}, \hat{y}\}}. \quad (36)$$

The transformation laws for the coherency matrix and the Stokes vector emerging from Eq. (36) are given by [44],

$$J \rightarrow J' \stackrel{\text{def}}{=} R_{\hat{z}}(\varphi_{\text{opt}}) \cdot J \cdot R_{\hat{z}}(-\varphi_{\text{opt}}), \quad (37)$$

and [45],

$$S \rightarrow S' \stackrel{\text{def}}{=} M_{\text{ROT}}(\varphi_{\text{opt}}) S = \mathcal{U} \cdot [R_{\hat{z}}^*(\varphi_{\text{opt}}) \otimes R_{\hat{z}}(\varphi_{\text{opt}})] \cdot \mathcal{U}^\dagger, \quad (38)$$

respectively, where  $\mathcal{U}$  is a  $(4 \times 4)$ -unitary matrix and  $M_{\text{ROT}}(\varphi_{\text{opt}})$  is a  $(4 \times 4)$ -Mueller matrix given by

$$\mathcal{U} \stackrel{\text{def}}{=} \frac{1}{\sqrt{2}} \begin{pmatrix} 1 & 0 & 0 & 1 \\ 1 & 0 & 0 & -1 \\ 0 & 1 & 1 & 0 \\ 0 & i & -i & 0 \end{pmatrix}, \text{ and } M_{\text{ROT}}(\varphi_{\text{opt}}) \stackrel{\text{def}}{=} \begin{pmatrix} 1 & 0 & 0 & 0 \\ 0 & \cos(2\varphi_{\text{opt}}) & \sin(2\varphi_{\text{opt}}) & 0 \\ 0 & -\sin(2\varphi_{\text{opt}}) & \cos(2\varphi_{\text{opt}}) & 0 \\ 0 & 0 & 0 & 1 \end{pmatrix}, \quad (39)$$

respectively. Imposing that  $J_{x'x'} = J_{y'y'}$ , from Eq. (37) we get that  $\varphi_{\text{opt}}$  is such that

$$\tan(2\varphi_{\text{opt}}) = \frac{J_{yy} - J_{xx}}{J_{xy} + J_{yx}}. \quad (40)$$

Since  $J_{xx}$ ,  $J_{yy}$ , and  $J_{xy} + J_{yx} = 2 \text{Re}(J_{xy}) \in \mathbb{R}$ , Eq. (40) has a real root. In conclusion, there always exists a pair of orthogonal directions  $\{\hat{x}', \hat{y}'\}$  with  $\hat{x}' \stackrel{\text{def}}{=} \hat{x} \cos \varphi_{\text{opt}} + \hat{y} \sin \varphi_{\text{opt}}$  and  $\hat{y}' \stackrel{\text{def}}{=} -\hat{x} \sin \varphi_{\text{opt}} + \hat{y} \cos \varphi_{\text{opt}}$  for which the two intensities  $J_{xx}$  and  $J_{yy}$  are equal. For this pair of directions, the degree of coherence  $|j_{xy}|$  reaches its maximum value  $|j_{xy}|_{\max}$  with  $|j_{xy}|_{\max} = P$ . This particular pair of directions  $\{\hat{x}', \hat{y}'\}$  has a neat geometric interpretation. Indeed, using Eqs. (32) and (40), it follows that

$$\tan(2\varphi_{\text{opt}}) \tan(2\chi) = -1, \quad (41)$$

that is,  $\varphi_{\text{opt}} - \chi = \pi/4$  or  $3\pi/4$ . Therefore, the directions  $\{\hat{x}', \hat{y}'\}$  for which  $\eta_{\text{opt}} \stackrel{\text{def}}{=} |j_{xy}|/P = 1$  are the bisectors of the principal directions  $\{\hat{\xi}, \hat{\eta}\}$  with  $\hat{\xi} \stackrel{\text{def}}{=} \hat{x} \cos \chi + \hat{y} \sin \chi$  and  $\hat{\eta} \stackrel{\text{def}}{=} -\hat{x} \sin \chi + \hat{y} \cos \chi$  of the polarization ellipse of the polarized portion of the wave [25]. Therefore, given that  $\hat{x}' = \hat{\xi} \cos(\varphi_{\text{opt}} - \chi) + \hat{\eta} \sin(\varphi_{\text{opt}} - \chi)$  and  $\hat{y}' = -\hat{\xi} \sin(\varphi_{\text{opt}} - \chi) + \hat{\eta} \cos(\varphi_{\text{opt}} - \chi)$  with  $\varphi_{\text{opt}} - \chi = \pi/4$  or  $3\pi/4$ , we have

$$\left| \hat{x}' \cdot \hat{\xi} \right| = \left| \hat{x}' \cdot \hat{\eta} \right| = \left| \hat{y}' \cdot \hat{\xi} \right| = \left| \hat{y}' \cdot \hat{\eta} \right| = 1/2, \quad (42)$$

since  $\hat{x}' = (\hat{\xi} + \hat{\eta})/\sqrt{2}$  and  $\hat{y}' = (\hat{\eta} - \hat{\xi})/\sqrt{2}$ . Observe that the optical conditions in Eq. (42) correspond to the quantum conditions

$$|\langle E_+ | A \rangle| = |\langle E_- | A \rangle| = |\langle E_+ | A_\perp \rangle| = |\langle E_- | A_\perp \rangle| = 1/2, \quad (43)$$

obtained when maximizing the energy uncertainty in Eq. (12). In Table III, we provide a schematic description of quantities of interest on the Bloch and the Poincaré spheres. In particular, we characterize the points  $P(\theta, \varphi)$  and  $P(\beta, \chi)$  on the two surfaces in terms of their spherical coordinates. Moreover, we specify the rotation operations yielding unit efficiency on the two spheres by means of their axes of rotation (that is,  $\hat{E}_+$  and  $\hat{z}$ , respectively) and their angles of rotation (that is,  $\cos^{-1}[|\langle A|B \rangle|]$  and  $\varphi_{\text{opt}}$ , respectively). Finally, we determine the two angles  $\varphi_{E_+}$  and  $\varphi_{\text{opt}}$  to be compared within the two geometric frameworks of unit efficiency quantum evolutions and unit efficiency polarized light propagation.

In the next section, we discuss the physical root that is underlying our proposed formal analogy.

Quantity of Interest	Bloch Sphere	Poincaré Sphere
angles	$(\theta, \varphi)$	$(\beta, \chi)$
range of angles	$0 \leq \theta \leq \pi, 0 \leq \varphi < 2\pi$	$-\pi/4 < \beta \leq \pi/4, 0 \leq \chi < \pi$
point on the sphere	$P(\theta, \varphi) \stackrel{\text{def}}{=} (\sin \theta \cos \varphi, \sin \theta \sin \varphi, \cos \theta)$	$P(\beta, \chi) \stackrel{\text{def}}{=} (\cos 2\beta \cos 2\chi, \cos 2\beta \sin 2\chi, \sin 2\beta)$
axis of rotation	$\hat{E}_+ = \hat{E}_+(\theta_{E_+}, \varphi_{E_+})$	$\hat{z}$ , fixed
angle of rotation	$\cos^{-1} [ \langle A B \rangle ]$ , fixed	$\varphi_{\text{opt}}$
angles to be compared	$\varphi_{E_+} = \varphi_{E_+}( A\rangle,  B\rangle)$	$\varphi_{\text{opt}} = \varphi_{\text{opt}}(P)$ , with $P = P(\beta, \chi)$

TABLE III: Schematic description of quantities of interest on the Bloch and the Poincaré spheres. In particular, we compare the description of points  $P(\theta, \varphi)$  and  $P(\beta, \chi)$  on the two surfaces in terms of their spherical coordinates. Moreover, we describe the rotation operations yielding unit efficiency on the two spheres in terms of their axes of rotation (that is,  $\hat{E}_+$  and  $\hat{z}$ , respectively) and their angles of rotation (that is,  $\cos^{-1} [|\langle A|B \rangle|]$  and  $\varphi_{\text{opt}}$ , respectively). Finally, we identify the two angles  $\varphi_{E_+}$  and  $\varphi_{\text{opt}}$  to be compared within the two geometric frameworks of unit efficiency quantum evolutions and polarization optics.

## V. PHYSICAL ORIGIN BEHIND THE FORMAL ANALOGY

The formal analogy between quantum evolutions with unit geometric efficiency and propagation of light with unit optical efficiency, discussed in this paper and summarized in Tables I and II, is yet another example of the close relationship that exists between certain classes of quantum mechanical and classical optical phenomena. Is this analogy completely unexpected? What is the physical reason that underlines such a formal similarity? This analogy is not completely unexpected. After all, as mentioned in the Introduction, Grover exploited his knowledge on the interference of classical light waves in order to construct his quantum search algorithm. Furthermore, the set of unit-speed quantum mechanical evolutions includes as a special case the Farhi-Gutmann search Hamiltonian [46], an analog version of Grover's digital quantum search scheme. Both Grover's and the Farhi-Gutmann search schemes rely heavily on the interference phenomenon for achieving their quadratic speedup. The phenomenon of interference, either constructive or destructive, plays a key role in both light propagation [43, 47] and quantum searching [48, 49]. For additional details on the role played by interference effects in light propagation, quantum searching, and optimal-speed quantum evolutions, we refer to Appendix D.

In what follows, we briefly discuss the role played by interference as the physical root underlying the formal analogy between propagation of light with maximal degree of coherence and optimal-speed unitary quantum propagation proposed in this paper.

### A. Interference of classical light waves

In the framework of coherent light propagation [43], two rays of light originating from the same source can interfere. Specifically, the two rays can be combined in such a manner to give rise to a light more intense than is ordinarily created by two light beams of their respective intensities (constructive interference). Alternatively, the superimposition of the two rays of light can yield a darkness (destructive interference). Therefore, coherent light propagation is characterized by interference effects where, in addition, the degree of coherence is equal to the degree of indistinguishability of the particle trajectories that yield the interference pattern [47]. When the photon pattern becomes identifiable, the interference effects disappear, and the light propagation becomes incoherent. In the study of coherence properties of partially polarized electromagnetic radiation [25], there is a proper angle that specifies a pair of directions for which the degree of coherence of the electric vibrations has its maximum value (which, in turn, equals the degree of polarization of the wave). As discussed in this paper, this angle  $\varphi_{\text{opt}}$  is determined by a specific value of the orientation angle  $\chi$  that characterizes the polarization ellipse used to describe the light propagation (see Eq. (41)).

From a more quantitative standpoint, consider a quasi-monochromatic light wave that propagates in the  $\hat{z}$ -direction specified by an electric field  $\vec{E}(t) = E_x(t)\hat{x} + E_y(t)\hat{y}$ . Assume that the component  $E_\theta = \vec{E} \cdot \hat{\theta}$  of the electric field in the  $\hat{\theta}$ -direction is given by,  $E_\theta(t; \theta, \varepsilon) \stackrel{\text{def}}{=} E_x(t) \cos(\theta) + E_y e^{i\varepsilon} \sin(\theta)$ , with  $\varepsilon$  denoting the phase delay between  $E_x$  and  $E_y$ . The interference law of light waves can be expressed by calculating the intensity  $I(\theta, \varepsilon)$  of the light vibrations in the direction which makes an angle  $\theta$  with the positive  $\hat{x}$ -direction. A straightforward calculation yields [25],

$$I(\theta, \varepsilon) = I_x + I_y + 2\sqrt{I_x}\sqrt{I_y}|j_{xy}|\cos(\beta_{xy} - \varepsilon). \quad (44)$$

In Eq. (44),  $I(\theta, \varepsilon) \stackrel{\text{def}}{=} \langle E_\theta(t; \theta, \varepsilon) E_\theta^*(t; \theta, \varepsilon) \rangle$  where sharp brackets denote time average,  $I_x \stackrel{\text{def}}{=} J_{xx} \cos^2(\theta)$ ,  $I_y \stackrel{\text{def}}{=} J_{yy} \sin^2(\theta)$ ,  $J_{ij}$  are the coefficients of the coherency matrix, and  $j_{xy} \stackrel{\text{def}}{=} |j_{xy}| e^{i\beta_{xy}}$  is the complex degree of coherence

of the electric vibrations in the  $\hat{x}$ - and  $\hat{y}$ -directions. Recall that  $|j_{xy}|$  in Eq. (44) is an indicator of the degree of correlation of the vibrations, while  $\beta_{xy}$  in Eq. (44) is an effective phase difference between the electric vibrations in the  $\hat{x}$ - and  $\hat{y}$ -directions. In modern terminology, we emphasize that  $J_{ij}$  are known as the coefficients of the polarization matrix [50]. Moreover, in the context of the classical theory of optical fluctuations and coherence, the analogue of  $|j_{xy}|$  is the so-called degree of first order coherence [51]. Regardless of notation and modern terminology, what is most important for us here is the contribution of  $j_{xy}$  with the interference term  $|j_{xy}| \cos(\beta_{xy} - \varepsilon)$  into the expression of the total intensity  $I(\theta, \varepsilon)$  in Eq. (44).

Interestingly, when studying the superposition of two coherent beams of light in different states of elliptic polarization, Pancharatnam showed in Ref. [10] that if  $A$  and  $B$  represent the states of polarization on the Poincaré sphere of the given interfering beams, and  $C$  that of the resultant beam, the intensity of the resultant beam can be recast as

$$I_C = I_A + I_B + 2\sqrt{I_A}\sqrt{I_B} \cos\left(\frac{\theta_{AB}^{\text{Poincaré}}}{2}\right) \cos(\delta). \quad (45)$$

In Eq. (45),  $\theta_{AB}^{\text{Poincaré}}$  is the angular separation of states  $A$  and  $B$  on the Poincaré sphere, while  $\delta$  is not quite the absolute difference of phase between the two beams and is defined as the phase advance of the first beam being in a state of polarization  $A$  over the  $A$ -component of the second beam being in a state of polarization  $B$ . If we set  $\varepsilon = \varepsilon_y$  in Eq. (44) and consider a nonvanishing phase  $\varepsilon_x$ ,  $\delta$  can be formally identified with  $\varepsilon_x - (\varepsilon_y - \beta_{xy})$ . For more details, we refer to Ref. [10].

## B. Interference of quantum probability amplitudes

In the framework of quantum searching viewed in the context of quantum computing as multi-particle interference [48, 49], the role of interference is fundamental since it permits the evolution from a source state to a target state by manipulating the intermediate multi-particle superpositions in a convenient way. Specifically, quantum searching can be regarded as inducing a proper relative phase between two eigenvectors to generate constructive interference on the searched elements and destructive interference on the remaining ones. As pointed out in this paper, this phase is quantified by a specific value of the azimuthal angle  $\varphi_{E_+}$  that specifies the location on the Bloch sphere of the eigenstates  $|E_{\pm}\rangle$  used to geometrically construct the optimal evolution (search) Hamiltonian  $H$ .

Therefore, interference appears to be the essential physical phenomenon that underlies both propagation of light with maximal degree of coherence and continuous-time quantum search evolution with minimum search time (i.e., optimal-speed). Interference is optimally exploited in the two above mentioned tasks so that unit optical and quantum efficiencies can be achieved by identifying suitable angles. These are the orientation and azimuthal angles in the optical and quantum search cases, respectively. The orientation angle  $\varphi_{\text{opt}}$  specifies the optimal unitary operation (Mueller rotation,  $M_{\text{ROT}}(\varphi_{\text{opt}})$ ) that connects the two initial and final polarization states on the Poincaré sphere. The azimuthal angle  $\varphi_{E_+}$ , instead, characterizes the optimal unitary operation (Bloch rotation,  $R_{\hat{E}_+}(\theta_{AB})$ ) with  $\theta_{AB} \stackrel{\text{def}}{=} \cos^{-1}[|\langle A|B\rangle|]$  and  $\hat{E}_+ \stackrel{\text{def}}{=} \hat{E}_+(\theta_{E_+}, \varphi_{E_+})$  that connects the source and the target states  $|A\rangle$  and  $|B\rangle$  on the Bloch sphere.

As mentioned earlier, the essential prerequisite for achieving speedups in quantum searching is interference of quantum probability amplitudes [52, 53]. This occurs in both Grover's original quantum search algorithm [31] and in the Farhi-Gutmann continuous version of Grover's algorithm [46]. Indeed, as pointed out by Lloyd in Ref. [32], Grover arrived at the formulation of his quantum search algorithm inspired by the interference of classical waves emitted by an array of antennae.

From an explicit viewpoint, consider a quantum state  $|\psi\rangle$  written as the superposition of two normalized quantum states  $|A\rangle$  and  $|B\rangle$  with complex probability amplitudes  $a \stackrel{\text{def}}{=} |a| e^{i\varphi_a}$  and  $b \stackrel{\text{def}}{=} |b| e^{i\varphi_b}$ , respectively, with  $\varphi_a$  and  $\varphi_b$  in  $\mathbb{R}$ . Furthermore, let us assume that  $\langle A|B\rangle = \langle B|A\rangle^* \stackrel{\text{def}}{=} |\langle A|B\rangle| e^{i\varphi_{AB}}$  with  $\varphi_{AB} \in \mathbb{R}$ . Then, the interference law of probability amplitudes  $a$  and  $b$  can be expressed in terms of their corresponding probabilities calculated by taking a modulus squared of the probability amplitudes. After some simple algebra in which we consider the inner product of  $|\psi\rangle$  with itself, the quantum interference law becomes

$$p_{a+b} = p_a + p_b + 2\sqrt{p_a}\sqrt{p_b} |\langle A|B\rangle| \cos[\varphi_{AB} - (\varphi_a - \varphi_b)], \quad (46)$$

where  $p_{a+b} \stackrel{\text{def}}{=} \langle \psi|\psi\rangle$ ,  $p_a \stackrel{\text{def}}{=} |a|^2$ , and  $p_b \stackrel{\text{def}}{=} |b|^2$ . In Eq. (46),  $|\langle A|B\rangle|$  can be viewed as  $\cos(\theta_{AB}^{\text{Bloch}}/2)$  with  $\theta_{AB}^{\text{Bloch}}$  being the geodesic distance on the Bloch sphere between the states  $|A\rangle$  and  $|B\rangle$ , while  $\varphi_a - \varphi_b$  is the absolute phase difference between the interfering probability amplitudes  $a$  and  $b$ . Interestingly, we remark the contribution of  $\langle A|B\rangle \stackrel{\text{def}}{=} |\langle A|B\rangle| e^{i\varphi_{AB}}$  with the interference term  $|\langle A|B\rangle| \cos[\varphi_{AB} - (\varphi_a - \varphi_b)]$  into the expression of the total probability  $p_{a+b}$  in Eq. (46).

Considering Eqs. (44), (45), and (46), we note that  $\langle A|B\rangle \stackrel{\text{def}}{=} |\langle A|B\rangle| e^{i\varphi_{AB}}$  corresponds to  $j_{xy} \stackrel{\text{def}}{=} |j_{xy}| e^{i\beta_{xy}}$ . In particular, we get

$$\frac{|J_{xy}|}{\sqrt{J_{xx}}\sqrt{J_{yy}}} \stackrel{\text{def}}{=} |j_{xy}| \leftrightarrow \cos\left(\frac{\theta_{AB}^{\text{Poincaré}}}{2}\right) \leftrightarrow \cos\left(\frac{\theta_{AB}^{\text{Bloch}}}{2}\right) \stackrel{\text{def}}{=} \frac{|\langle A|B\rangle|}{\sqrt{\langle A|A\rangle}\sqrt{\langle B|B\rangle}}. \quad (47)$$

Eq. (47) is especially relevant since the degree of correlation of the electric vibrations ( $|j_{xy}|$ ) viewed in terms of the angular separation on the Poincaré sphere ( $\theta_{AB}^{\text{Poincaré}}$ ) can be regarded as corresponding to the geodesic distance on the Bloch sphere ( $\theta_{AB}^{\text{Bloch}}$ ). In the analysis carried out in our paper, both  $\cos(\theta_{AB}^{\text{Bloch}}/2)$  and  $|j_{xy}|$  played a major role in the proposed definitions of quantum geometric efficiency  $\eta_{\text{QM}} \stackrel{\text{def}}{=} s_0/s$  and classical optical efficiency  $\eta_{\text{opt}} \stackrel{\text{def}}{=} |j_{xy}|/P$ .

In summary, we have discussed the link between propagation of light with maximal degree of coherence and optimal-speed quantum propagation by performing a punctual comparative analysis of geometric flavor. The emergence of this formal analogy is physically motivated by the existence of a key physical phenomenon that underlies both types of evolutions at their best, i.e., interference. This link among  $|j_{xy}|$ ,  $\theta_{AB}^{\text{Poincaré}}$ , and  $\theta_{AB}^{\text{Bloch}}$  in Eq. (47) that emerges while thinking of interference of classical waves (classical optics) and interference of probability amplitudes (quantum mechanics) should be kept in mind as a constant (hidden) theme underlying our discussion in the main paper.

## VI. CONCLUDING REMARKS

We present here a summary of our main findings along with a discussion on possible future applications of our work.

### A. Summary of results

In this paper, we identified and discussed in a quantitative manner a link between the geometry of time-independent optimal-speed Hamiltonian quantum evolutions on the Bloch sphere and the geometry of intensity-preserving propagation of light with maximal degree of coherence on the Poincaré sphere.

Specifically, we carried out a detailed comparative analysis between the quantum and optical scenarios. In the quantum case, we focused on the main constraint equations (Eqs. (2) and (13)) leading to the construction of the optimal unitary evolution operator  $e^{-\frac{i}{\hbar}HT_{AB}}$  (that is, a rotation of a Bloch vector on the Bloch sphere) with the optimal Hamiltonian given in Eqs. (11) and (19). In the optical case, similarly, we focused on the main constraint equations (Eqs. (34) and (35)) leading to the construction of the optimal Mueller matrix  $M_{\text{ROT}}(\varphi_{\text{opt}})$  (see Eq. (39) with  $\varphi_{\text{opt}}$  in Eq.(40). This Mueller matrix acts on a Stokes vector on the Poincaré sphere (see Eq. (38)) and leads to the propagation of light with maximal degree of coherence in analogy to the geodesic path defined in Eq. (20) and generated by the Hamiltonian in Eq. (19). In particular, in Table I we presented an explicit correspondence between the main quantum and optical quantities that enter the two phenomena. In Table II, we pointed out the two main constraint relations that specify the two physical scenarios. Finally, in Table III, we concluded with the correspondence between axes and angles of rotations that specify the two optimal operations yielding unit quantum geometric efficiency and classical optical efficiency, respectively.

Our main achievement in this paper is bringing to light this fascinating analogy between optimal-speed quantum evolutions and polarized light propagation with maximal degree of coherence. This link was never noticed before and, to the best of our knowledge, it constitutes a new connection between the quantum physics of two-level systems and classical polarization optics. To a certain extent, we think that our investigation is not only relevant from a pure theoretical perspective, it can also be regarded (in retrospect) as providing a sort of conceptual and quantitative geometric background underlying Grover's powerful intuition about constructing a quantum search scheme by mimicking interference of classical waves [32].

Clearly, it could be worthwhile exploring the possibility of extending our work to higher-dimensional quantum systems since a single two-level quantum system is so simple that connecting it to classical wave propagation may not necessarily make the two-level system more intuitive. A richer Hilbert space structure would be more appropriate to fully gain physical insights emerging from our proposed analogy. Therefore, we expect that it would be very helpful outlining the needed formalism to generalize our current result to multi-qubits quantum systems and demonstrate, for instance, that classical optics is an intuitive way to understand entangled quantum systems. This is a crucial step that we leave to future scientific efforts since it goes beyond the scope of the paper. However, in the next subsection, we do explore in a qualitative manner some possible future line of investigations that emerge from our analysis.

## B. Outlook

In addition to its intrinsic conceptual and pedagogical values, our theoretical study paves the way to several intriguing explorative physics questions that require more attention.

- First, regarding the time-optimal Hamiltonian analysis within the general setting specified by the so-called quantum brachistochrone problem (QBP, [54, 55]), it may be of interest investigating similarities between propagation of light with maximal degree of coherence and the QBP. In this context, one may think of extending our investigation to higher-dimensional spin systems [56] and to constraint equations specifying cost functions other than time-optimality [57, 58]. In our paper, we have provided the optical analogue of a QBP via its analogy with the propagation of light with maximal degree of coherence. The QBP was characterized by a cost functional defined in terms of time-optimality to be optimized by imposing a single constraint, a bound on the energy resource. In general, defining the cost functional, an efficiency measure of getting to a target state from a given initial state by a suitable choice of a Hamiltonian, is a nontrivial task that depends on the physical scenario being investigated. As pointed out in the Introduction, there is a variety of cost functionals that one may consider in QBPs and, in addition, the optimization procedure may be specified by multiple constraints to be simultaneously satisfied. A typical set of examples includes minimization of the total amount of time [54], the heating rate [6], the energy dispersion rate [6], and the entropy production rate [59, 60]. It would be certainly interesting from a physics perspective uncovering possible optical analogues of such more general QBPs. We think that identifying suitable optical constraints would be a key step in this direction and one may need to go beyond considering constraints expressed in terms of the intensity of light.
- Second, being in the framework of quantum speed limit (QSL) problems concerning the minimum time needed to transfer a given initial quantum state to a final one [61–63], it appears that changes in coherence have significant dynamical effects on the evolution speeds of the reduced state of certain families of quantum gases viewed as interacting many-particle systems [64]. More specifically, in Ref. [64] the authors study the dynamics of the reduced single-particle density matrix (RSPDM) of a strongly correlated bosonic quantum gas in one dimension and a gas of spinless fermions. They focus on two dynamical processes, a sudden quench, and the efficient control of the system by means of a shortcut to adiabaticity. The physics of the gases is characterized in terms of the time-averaged Schatten-1 norm of the dynamics, that is the speed of evolution of the system. Furthermore, the coherence of the gases is specified by means of the largest eigenvalue of the RSPDM, a good measure of the presence of off-diagonal long-range order. The authors state in Ref. [64] that coherences play an essential role in the evolution of the reduced state of the systems. In the case of strongly interacting bosons, they find larger average speeds (thus, smaller quantum speed limit times) due to the presence of off-diagonal excitations emerging from the scattering between particles. In our work, the minimum quantum speed limit time is achieved in the presence of maximal energy dispersion with the speed of evolution of the quantum system being proportional to the energy dispersion of the Hamiltonian operator. Furthermore, our results suggest that maximal energy dispersion corresponds from an optical standpoint to maximal correlations between the orthogonal electric field components of the light wave that appear as off-diagonal terms in the coherency matrix. Thus, the minimum quantum speed limit time appears to correspond to a maximal correlational structure in the field components specifying the electromagnetic radiation. Given these formal similarities between our work and the one in Ref. [64], it seems rather intriguing exploring if our analysis might help further understanding the role played by coherence in the control of many-body quantum states. We believe that a first significant step in this direction would be exploring the possible existence of a quantitative connection between the degree of coherence employed in our work and the coherence specified by means of the largest eigenvalue of the RSPDM.
- Third, when studying quantum resources, it happens that the quantum Fisher information and the super-radiant quantity attributed to coherence are antithetical resources. Specifically, there is a trade-off between the quantum Fisher information and the super-radiant quantity [65]. The trade-off emerges in a coherence limited scenario where optimizing one quantity seems to suggest less quantum resources that can be utilized for the other. Interestingly, identifying the energy uncertainty and the degree of coherence with the quantum Fisher information and the super-radiant quantity, respectively, we also find there appears to be a conflicting behavior between these two quantities. Indeed, considering the unit efficiency scenario where time-optimality is the resource to be optimized, to an increase of one of these two quantities there corresponds necessarily a decrease of the other one for a fixed minimum total amount of time for the evolution. To further elaborate on this point, we remark that in Ref. [66] the authors study the Dicke model of superradiance specified by a system of  $N$  identical two-level atoms with transition frequency  $\omega$  and interacting in a collective fashion with the surrounding electromagnetic field in the vacuum state at zero temperature. They find that the  $l_1$  norm of coherence of the single-atom density operator is proportional to the square root of the normalized average

radiation intensity emitted in a cooperative manner by the whole superradiant system. This radiation intensity, in turn, can be recast in terms of the coherence of the normalized total electric dipole moment of the system. Thus, an important link between the  $l_1$  norm of coherence of the single-atom density operator and the coherence of the normalized total electric dipole moment of the system is emphasized. This link leads to the validation of the  $l_1$  norm of coherence as a figure of merit of the superradiance phenomenon in the mean-field approach. As a main finding, the authors showed that the evolution of the system is faster when more coherence is stored in the single-atom state. Interestingly, our investigation also leads to the conclusion that optimal evolution speed corresponds to maximal degree of coherence. Our work could be potentially relevant for better understanding the reason why quantum coherence speeds up the evolution of superradiant systems. We anticipate that a basic preliminary step in this direction would be that of clarifying the relation between the degree of coherence employed in our work and the  $l_1$  norm of coherence, a very intuitive and easy to use coherence measure related to off-diagonal elements of a quantum state with the key feature of being the most general coherence monotone introduced in Ref. [67] and discussed with emphasis on its applications in Ref. [68].

- Fourth, it is pointed out in Ref. [68] that quantum coherence can also be used as a resource in quantum algorithms. For instance, it is emphasized that the success probability in the analog Grover algorithm depends on the amount of coherence, quantified via the  $l_1$  norm of coherence, in the corresponding quantum state [69, 70]. Uncovering possible links between our current work and the findings presented in Refs. [69, 70] could be yet another intriguing avenue to explore in future investigations. Given the physically intuitive link with off-diagonal elements of both the  $l_1$  norm of coherence and the degree of coherence used in our work, we remark once again that a much needed step in this direction would be investigating the possibility of quantifying light propagation by means of the  $l_1$  norm of coherence.

We hope our work will inspire other scientists and pave the way toward further investigations in this fascinating research direction. For the time being, we leave a more in-depth quantitative discussion on these potential extensions and applications of our theoretical findings to quantum brachistochrone problems, quantum speed limits questions, and quantum resources analyses to future scientific efforts.

### Acknowledgments

C.C. is grateful to the United States Air Force Research Laboratory (AFRL) Summer Faculty Fellowship Program for providing support for this work. S.R. acknowledges support from the National Research Council Research Associate Fellowship program (NRC-RAP). P.M.A. acknowledges support from the Air Force Office of Scientific Research (AFOSR). Any opinions, findings and conclusions or recommendations expressed in this material are those of the author(s) and do not necessarily reflect the views of the Air Force Research Laboratory (AFRL). The Authors thank the anonymous Referees for stimulating comments leading to an improved version of the manuscript.

- 
- [1] T. Caneva, M. Murphy, T. Calarco, R. Fazio, S. Montagero, V. Giovannetti, and G. E. Santoro, *Optimal control at the quantum speed limit*, Phys. Rev. Lett. **103**, 240501 (2009).
  - [2] V. Mukherjee, A. Carlini, A. Mari, T. Caneva, S. Montagero, T. Calarco, R. Fazio, and V. Giovannetti, *Speeding up and slowing down the relaxation of a qubit by optimal control*, Phys. Rev. **A88**, 062326 (2013).
  - [3] G. C. Hegerfeldt, *Driving at the quantum speed limit: Optimal control of a two-level system*, Phys. Rev. **111**, 260501 (2013).
  - [4] U. Boscain, M. Sigalotti, and D. Sugny, *Introduction to the Pontryagin maximum principle for quantum optimal control*, PRX Quantum **2**, 030203 (2021).
  - [5] D. C. Brody, G. W. Gibbons, and D. M. Meier, *Time-optimal navigation through quantum wind*, New J. Phys. **17**, 033048 (2015).
  - [6] S. Deffner, *Optimal control of a qubit in an optimal cavity*, J. Phys. B: At. Mol. Opt. Phys. **47**, 145502 (2014).
  - [7] U. Fano, *A Stokes-parameter technique for the treatment of polarization in quantum mechanics*, Phys. Rev. **93**, 121 (1954).
  - [8] M. A. Nielsen and I. L. Chuang, *Quantum Computation and Quantum Information*, Cambridge University Press (2000).
  - [9] M. Born and E. Wolf, *Principles of Optics*, Cambridge University Press (2003).
  - [10] S. Pancharatnam, *Generalized theory of interference, and its applications*, Proc. Ind. Acad. Sci. **A44**, 247 (1956).
  - [11] M. V. Berry, *Quantal phase factors accompanying adiabatic changes*, Proc. R. Soc. Lond. **A392**, 45 (1984).
  - [12] M. V. Berry, *The adiabatic phase and Pancharatnam's phase for polarized light*, J. Mod. Opt. **34**, 1401 (1987).
  - [13] J. Samuel and R. Bhandari, *General setting for Berry's phase*, Phys. Rev. Lett. **60**, 2339 (1988).
  - [14] R. Y. Chiao and Y.-S. Wu, *Manifestation of Berry's topological phase for the photon*, Phys. Rev. Lett. **57**, 933 (1986).

- [15] T. F. Jordan, *Direct calculation of the Berry phase for spins and helicities*, J. Math. Phys. **28**, 1759 (1987).
- [16] H. Moya-Cessa, J. R. Moya-Cessa, J. E. A. Landgrave, G. Martinez-Niconoff, A. Perez-Leija, and A. T. Friberg, *Degree of polarization and quantum-mechanical purity*, J. Eur. Opt. Soc. Rap. Public. **3**, 08014 (2008).
- [17] O. Gamel and D. F. V. James, *Measures of quantum state purity and classical degree of polarization*, Phys. Rev. **A86**, 033830 (2012).
- [18] C. M. Bender, D. C. Brody, H. F. Jones, and B. K. Meister, *Faster than Hermitian quantum mechanics*, Phys. Rev. Lett. **98**, 040403 (2007).
- [19] A. Mostafazadeh, *Hamiltonians generating optimal-speed evolutions*, Phys. Rev. **A79**, 014101 (2009).
- [20] D. C. Brody and D. W. Hook, *On optimum Hamiltonians for state transformations*, J. Phys. A: Math. Gen. **39**, L167 (2006).
- [21] D. C. Brody and D. W. Hook, *On optimum Hamiltonians for state transformation*, J. Phys. A: Math. Theor. **40**, 10949 (2007).
- [22] D. C. Brody, *Elementary derivation for passage times*, J. Phys. A: Math. Gen. **36**, 5587 (2003).
- [23] J. Anandan and Y. Aharonov, *Geometry of quantum evolution*, Phys. Rev. Lett. **65**, 1697 (1990).
- [24] C. Cafaro, S. Ray, and P. M. Alsing, *Geometric aspects of analog quantum search evolutions*, Phys. Rev. **A102**, 052607 (2020).
- [25] E. Wolf, *Coherence properties of partially polarized electromagnetic radiation*, Il Nuovo Cimento **13**, 1180 (1959).
- [26] C. Cafaro, *Geometric algebra and information geometry for quantum computational software*, Physica **A470**, 154 (2017).
- [27] C. Cafaro and P. M. Alsing, *Theoretical analysis of a nearly optimal analog quantum search*, Physica Scripta **94**, 085103 (2019).
- [28] C. Cafaro and P. M. Alsing, *Continuous-time quantum search and time-dependent two-level quantum systems*, Int. J. Quantum Information **17**, 1950025 (2019).
- [29] S. Gassner, C. Cafaro, and S. Capozziello, *Transition probabilities in generalized quantum search Hamiltonian evolutions*, Int. J. Geom. Meth. Mod. Phys. **17**, 2050006 (2020).
- [30] C. Cafaro, D. Felice, and P. M. Alsing, *Quantum Groverian geodesic paths with gravitational and thermal analogies*, Eur. Phys. J. Plus **135**, 900 (2020).
- [31] L. K. Grover, *Quantum mechanics helps in searching for a needle in a haystack*, Phys. Rev. Lett. **79**, 325 (1997).
- [32] S. Lloyd, *Quantum search without entanglement*, Phys. Rev. **A61**, 010301(R) (1999).
- [33] Note that our Eq. (11) fixes a typographical error that appears in Eq. (6) of Ref. [18]. As a cross check, we also verified that our Hamiltonian in Eq. (11) satisfies the correct maximal energy dispersion relation  $\Delta E = \Delta E_{\max} \stackrel{\text{def}}{=} (E_+ - E_-)/2 = E_0/2$  with  $E_+ - E_- \stackrel{\text{def}}{=} E_0 = \text{fixed}$ .
- [34] Observe that our Eq. (18) fixes a typographical error that appears in Eq. (12) of Ref. [19]. As a cross check, we also verified that our Hamiltonian in Eq. (18) satisfies the correct maximal energy dispersion relation given by  $\Delta E = \Delta E_{\max} \stackrel{\text{def}}{=} (E_+ - E_-)/2 = E$  with  $E_+ = -E_- \stackrel{\text{def}}{=} E$ .
- [35] S. Chandrasekhar, *Radiative Transfer*, Clarendon Press (1950).
- [36] E. Collett, *The description of polarization in classical physics*, Am. J. Phys. **36**, 713 (1968).
- [37] M. J. Walker, *Matrix calculus and the Stokes parameters of polarized radiation*, Am. J. Phys. **22**, 170 (1954).
- [38] R. C. Jones, *A new calculus for the treatment of optical systems. I. Description and discussion of the calculus*, J. Opt. Soc. Am. **31**, 488 (1941); R. C. Jones, *A new calculus for the treatment of optical systems. IV*, J. Opt. Soc. Am. **32**, 486 (1942).
- [39] H. Mueller, *The foundation of optics*, J. Opt. Soc. Am. **38**, 661 (1948).
- [40] G. Stokes, *On the composition and resolution of streams of polarized light from different sources*, Trans. Cambridge Phil. Soc. **9**, 399 (1852).
- [41] F. Perrin, *Polarization of light scattered by isotropic opalescent media*, J. Chem. Phys. **10**, 415 (1942).
- [42] H. Poincaré, *Traité de la Lumière*, Paris **2**, 165 (1892).
- [43] N. Wiener, *Generalized harmonic analysis*, Acta Math. **55**, 117 (1930).
- [44] S. Baskal, Y. S. Kim, and M. E. Noz, *Mathematical Devices for Optical Sciences*, IOP Publishing Ltd (2019).
- [45] R. A. Chipman, W.-S. Tiffany Lam, and G. Young, *Polarized Light and Optical Systems*, CRC Press (2019).
- [46] E. Farhi and S. Gutmann, *Analog analogue of a digital quantum computation*, Phys. Rev. **A57**, 2403 (1998).
- [47] L. Mandel, *Coherence and indistinguishability*, Optics Letters **16**, 1882 (1991).
- [48] R. Cleve, A. Ekert, L. Henderson, C. Macchiavello, and M. Mosca, *On quantum algorithms*, Complexity **4**, 33 (1998).
- [49] R. Cleve, A. Ekert, C. Macchiavello, and M. Mosca, *Quantum algorithms revisited*, Proc. Roy. Soc. Lond. **A454**, 339 (1998).
- [50] E. Wolf, *Introduction to the Theory of Coherence and Polarization of Light*, Cambridge University Press (2007).
- [51] R. Loudon, *The Quantum Theory of Light*, Oxford University Press (2000).
- [52] A. Ekert and R. Jozsa, *Quantum computation and Shor's factoring algorithm*, Rev. Mod. Phys. **68**, 733 (1996).
- [53] A. Galindo and M. A. Martin-Delgado, *Information and computation: classical and quantum aspects*, Rev. Mod. Phys. **74**, 347 (2002).
- [54] A. Carlini, A. Hosoya, T. Koike, and Y. Okudaira, *Time-optimal quantum evolution*, Phys. Rev. Lett. **96**, 060503 (2006).
- [55] F. Campaioli, W. Sloan, K. Modi, and F. A. Pollock, *Algorithm for solving unconstrained unitary quantum brachistochrone problems*, Phys. Rev. **A100**, 062328 (2019).
- [56] A. M. Frydryszak and V. M. Tkachuk, *Quantum brachistochrone problem for a spin-1 system in a magnetic field*, Phys. Rev. **A77**, 014103 (2008).

- [57] B. Russell and S. Stepney, *Zarmelo navigation and a speed limit to quantum information processing*, Phys. Rev. **A90**, 012303 (2014).
- [58] B. Russell and S. Stepney, *Zarmelo navigation in the quantum brachistochrone*, J. Phys. A: Math. Theor. **48**, 115303 (2015).
- [59] C. Cafaro and P. M. Alsing, *Information geometry aspects of minimum entropy production paths from quantum mechanical evolutions*, Phys. Rev. **E101**, 022110 (2020).
- [60] S. Gassner, C. Cafaro, S. A. Ali, and P. M. Alsing, *Information geometric aspects of probability paths with minimum entropy production for quantum state evolution*, Int. Geom. Meth. Mod. Phys. **18**, 2150127 (2021).
- [61] L. Mandelstam and I. G. Tamm, *The uncertainty relation between energy and time in non-relativistic quantum mechanics*, J. Phys. USSR **9**, 249 (1945).
- [62] N. Margolus and L. B. Levitin, *The maximal speed of dynamical evolution*, Physica **D120**, 188 (1998).
- [63] S. Deffner and S. Campbell, *Quantum speed limits: From Heisenberg's uncertainty principle to optimal quantum control*, J. Phys. A: Math. Theor. **50**, 453001 (2017).
- [64] T.-N. Xu, J. Li, T. Busch, X. Chen, and T. Fogarty, *Effects of coherence on quantum speed limits and shortcuts to adiabaticity in many-particle systems*, Phys. Rev. Research **2**, 023125 (2020).
- [65] K. C. Tan, S. Choi, H. Kwon, and H. Jeong, *Coherence, quantum Fisher information, superradiance, and entanglement as interconvertible resources*, Phys. Rev. **A97**, 052304 (2018).
- [66] D. Z. Rossatto, D. P. Pires, F. M. de Paula, and O. P. de Sa Neto, *Quantum coherence and speed limit in the mean-field Dicke model of superradiance*, Phys. Rev. **A102**, 05716 (2020).
- [67] T. Baumgratz, M. Cramer, and M. B. Plenio, *Quantifying coherence*, Phys. Rev. Lett. **113**, 140401 (2014).
- [68] A. Streltsov, G. Adesso, and M. B. Plenio, *Colloquium: Quantum coherence as a resource*, Rev. Mod. Phys. **89**, 04103 (2017).
- [69] N. Anand and A. K. Pati, *Coherence and entanglement monogamy in the discrete analogue of analog Grover search*, arXiv: quant-ph/1611.04542 (2016).
- [70] H.-L. Shi, S.-Y. Liu, X.-H. Wang, W.-L. Yang, Z.-Y. Yang, and H. Fan, *Coherence depletion in the Grover quantum search algorithm*, Phys. Rev. **A95**, 032307 (2017).
- [71] R. C. Jones, *A new calculus for the treatment of optical systems V. A more general formulation, and description of another calculus*, J. Opt. Soc. Am. **37**, 107 (1947).
- [72] A. Z. Goldberg, *Quantum theory of polarimetry: From quantum operations to Mueller matrices*, Phys. Rev. Research **2**, 023038 (2020).
- [73] D. G. Anderson and R. Barakat, *Necessary and sufficient conditions for a Mueller matrix to be derivable from a Jones matrix*, J. Opt. Soc. Am. **A11**, 2305 (1994).
- [74] S.-Y. Lu and R. A. Chipman, *Interpretation of Mueller matrices based on polar decomposition*, J. Opt. Soc. Am. **A13**, 1106 (1996).
- [75] L. H. Ryder, *Quantum Field Theory*, Cambridge University Press (1996).
- [76] E. P. Wigner, *Group Theory and its Applications to Quantum Mechanics*, Academic Press, New York (1959).
- [77] S. R. Cloude, *Group theory and polarisation algebra*, Optik **75**, 26 (1986).
- [78] T. Qureshi, *Coherence, interference and visibility*, Quanta **8**, 24 (2019).
- [79] X. Wang, M. Allegra, K. Jacobs, S. Lloyd, C. Lupo, and M. Mohseni, *Quantum brachistochrone curves as geodesics: Obtaining accurate minimum-time protocols for the control of quantum systems*, Phys. Rev. Lett. **114**, 170501 (2015).

## Appendix A: Mueller matrices

In this Appendix, we provide further details on the Mueller matrices mentioned in subsection B of Section III. Furthermore, we devote special emphasis on their relation with the Jones matrices. Finally, we emphasize how points on the surface of the Poincaré sphere are rotated by means of specific types of Mueller matrices.

In the traditional approach to polarization optics, the light propagates along the  $\hat{z}$ -axis and one considers the electric vector field components along the  $\hat{x}$ - and  $\hat{y}$ -directions. The polarization state is determined by the amplitude ratio and phase difference of the electric field components. Therefore, polarization can be modified either by changing the amplitudes or by tuning the relative phases, or both. Within the Jones calculus [38, 71], the Jones vector in  $\mathbb{C}^2$  represents the polarized light by means of the amplitude and the phase of the electric field in the  $\hat{x}$ - and  $\hat{y}$ -directions. Furthermore, linear optical elements (for instance, beam splitters, lenses, and mirrors) are represented by  $2 \times 2$  Jones matrices. Within the Mueller calculus [39], employing the concepts of Stokes parameters and Poincaré sphere, the change of polarization due to the interaction of light with an optical device can be described by the action of a  $4 \times 4$  matrix that represents a linear transformation acting upon a  $4 \times 1$  matrix corresponding to the Stokes vector. Within the Mueller calculus, there are three fundamental optical elements: wave plates, rotators, and polarizers. A wave plate and a rotator produce phase shifts and rotations of the Stokes vector, respectively. They are described by unitary matrices since they do not change the intensity of the light. Polarizers cause anisotropic attenuation and do change the intensity of light passing through them. Therefore, unlike wave plates and rotators, they are described by nonunitary matrices. The matricial representation of optical devices is very useful. Indeed, the composite effect of a series of

optical devices crossed by a light beam is represented by the product of the matrices corresponding to the various optical elements in the series. Mueller matrices can be grouped into two main categories [72]: Nondepolarizing and depolarizing Mueller matrices. Nondepolarizing Mueller matrices can modify the degree of polarization of partially polarized light. However, they do not change the degree of polarization of perfectly polarized light. Depolarizing Mueller matrices, instead, while maintaining the total intensity of the light beam, do reduce the degree of polarization of completely polarized light. Furthermore, nondepolarizing Mueller matrices have equivalent Jones matrices. On the other hand, depolarizing Mueller matrices have no equivalent Jones matrices. For a discussion on necessary and sufficient conditions for a Mueller matrix to be derivable from a Jones matrix, we refer to Ref. [73]. Interestingly, it is possible to show that any Mueller matrix can be decomposed into a sequence of three matrix factors [74]: a diattenuator, followed by a retarder, then followed by a depolarizer. Diattenuators and retarders are described by Hermitian Jones matrices and change only the amplitudes of the components of the electric field vector. A polarizer is an example of a diattenuator. Retarders, instead, are described by unitary Jones matrices and change only the phases of components of the electric field vector. A wave plate is an example of a retarder. As mentioned earlier, there are Mueller matrices with no corresponding Jones matrices. However, it turns out that any Jones matrix  $J$  acting on the electric field  $\vec{E}$  can be transformed into the corresponding Mueller matrix  $M$  given by  $M \stackrel{\text{def}}{=} A(J \otimes J^*)A^{-1}$ , where “ $*$ ” and “ $\otimes$ ” denote the complex conjugate and the tensor product, respectively. Moreover,  $A$  is a  $4 \times 4$  matrix defined as,

$$A \stackrel{\text{def}}{=} \begin{pmatrix} 1 & 0 & 0 & 1 \\ 1 & 0 & 0 & -1 \\ 0 & 1 & 1 & 0 \\ 0 & -i & i & 0 \end{pmatrix}. \quad (\text{A1})$$

Observe that the four rows  $\{R_A^i\}_{1 \leq i \leq 4}$  of  $A$  in Eq. (A1) are given by the coefficients of the identity matrix  $I$  and the three Pauli matrices  $\{\sigma_x, \sigma_y, \sigma_z\}$  with  $R_A^1 \leftrightarrow I$ ,  $R_A^2 \leftrightarrow \sigma_z$ ,  $R_A^3 \leftrightarrow \sigma_x$ , and  $R_A^4 \leftrightarrow \sigma_y$ . It is well-known that there is a two-to-one homomorphism between the complex special unitary group  $SU(2)$  and the real group of three-dimensional pure rotations  $O^+(3)$  [75],

$$SU(2) \ni e^{i\vec{\sigma} \cdot \hat{n} \frac{\theta}{2}} \leftrightarrow e^{i\vec{J} \cdot \hat{n} \theta} \in O^+(3). \quad (\text{A2})$$

In Eq. (A2),  $\hat{n}$  denotes the axis of rotation,  $\theta$  is the angle of rotation,  $\vec{\sigma} \stackrel{\text{def}}{=} (\sigma_1, \sigma_2, \sigma_3)$  is the Pauli matrix vector, and  $\vec{J} \stackrel{\text{def}}{=} (J_1, J_2, J_3)$  is the generator vector for  $O^+(3)$ . Interestingly, it can be shown that the matrix coefficients  $R_{ij}$  of any rotation matrix  $R$  in  $O^+(3)$  can be recast as [76],

$$R_{ij} = \frac{1}{2} \text{tr}(U^\dagger \cdot \sigma_i \cdot U \cdot \sigma_j), \quad (\text{A3})$$

where  $U$  is a two-dimensional unitary matrix with determinant equal to one specified by three free (real) parameters. From Eqs. (A2) and (A3), we note there is a global topological difference between  $SU(2)$  and  $O^+(3)$ . For example, increasing the angle  $\theta$  by  $2\pi$  in Eq. (A2), we get  $U \rightarrow -U$  in  $SU(2)$  while  $R \rightarrow R$  in  $O^+(3)$ . Therefore, both  $U$  and  $-U$  in  $SU(2)$  correspond to the same  $R$  in  $O^+(3)$ . Thus, there exists a two-to-one mapping of elements of  $SU(2)$  onto  $O^+(3)$ . Exploiting the  $SU(2)$ - $O^+(3)$  homomorphism, it happens that to a  $SU(2)$  matrix  $U$  acting on the vector field  $\vec{E}$  there corresponds a  $4 \times 4$  Mueller matrix viewed as an augmented form of a  $O^+(3)$  matrix  $R$  [77],

$$M \stackrel{\text{def}}{=} \begin{pmatrix} 1_{1 \times 1} & O_{1 \times 3} \\ O_{3 \times 1} & R_{3 \times 3} \end{pmatrix}, \quad (\text{A4})$$

where the coefficients  $M_{ij}$  of the matrix  $M$  are given by,

$$M_{ij} \stackrel{\text{def}}{=} \frac{1}{2} \text{tr}(U^\dagger \cdot \Xi_i \cdot U \cdot \Xi_j), \quad (\text{A5})$$

with  $\Xi \stackrel{\text{def}}{=} (I, \sigma_z, \sigma_x, \sigma_y)$ . For completeness, we remark that Eq. (A5) can also be extended by considering arbitrary complex (scattering) matrices  $U_{\text{complex}}$  in place of  $SU(2)$  matrices. In this case, the effect of the Mueller matrix with coefficients  $M_{ij} \stackrel{\text{def}}{=} 1/2 \text{tr}(U_{\text{complex}}^\dagger \cdot \Xi_i \cdot U_{\text{complex}} \cdot \Xi_j)$  is to combine a rotation of the Stokes vector with a change of its length (which, in turn, corresponds to a change in the degree of polarization). For more details on polarization algebra with Mueller matrices, we refer to Ref. [77].

## Appendix B: Degree of coherence of partially polarized waves

In this Appendix, we use the Poincaré sphere formalism to describe the behavior of the modulus  $|j_{xy}|$  of the complex degree of coherence  $j_{xy}$  of partially polarized light beams in terms of the ellipticity and orientation angles. Appendix B helps better understanding the content of subsection B of Section III with regard to partially polarized light waves with  $P < 1$ .

Partially polarized waves can be regarded as points that are inside the Poincaré sphere of radius  $I_{\text{tot}}$  (i.e., the total intensity of the wave) and at a distance  $I_{\text{pol}}$  (i.e., the intensity of the polarized part of the wave) from the origin of the sphere itself. Using the Stokes parameters  $\{S_0, S_1, S_2, S_3\}$ , we note that the degree of polarization  $P$  and  $|j_{xy}|$  can be recast as,

$$P = \frac{(S_1^2 + S_2^2 + S_3^2)^{1/2}}{S_0}, \text{ and } |j_{xy}| = \left( \frac{S_2^2 + S_3^2}{S_0^2 - S_1^2} \right)^{1/2}, \quad (\text{B1})$$

respectively. From Eq. (B1), we have that if  $S_0^2 = S_1^2 + S_2^2 + S_3^2$  then  $P = |j_{xy}| = 1$ . Instead, if  $S_0^2 > S_1^2 + S_2^2 + S_3^2$  then  $P < 1$  and  $|j_{xy}| \leq P$ . Furthermore, using the two relations in Eq. (B1) along with setting  $S_0 \stackrel{\text{def}}{=} I_{\text{tot}}$ ,  $S_1 \stackrel{\text{def}}{=} I_{\text{pol}} \cos(2\beta) \cos(2\chi)$ ,  $S_2 \stackrel{\text{def}}{=} I_{\text{pol}} \cos(2\beta) \sin(2\chi)$ , and  $S_3 \stackrel{\text{def}}{=} I_{\text{pol}} \sin(2\beta)$ , we get

$$|j_{xy}| = |j_{xy}(\beta, \chi; P) \stackrel{\text{def}}{=} P \left[ \frac{1 - \cos^2(2\beta) \cos^2(2\chi)}{1 - P^2 \cos^2(2\beta) \cos^2(2\chi)} \right]^{1/2}, \quad (\text{B2})$$

where  $P \stackrel{\text{def}}{=} I_{\text{pol}}/I_{\text{tot}}$ ,  $-\pi/4 < \beta \leq \pi/4$ , and  $0 \leq \chi < \pi$ . Finally, we note from Eq. (B2) that for a given value of  $P < 1$  and for any value of the ellipticity angle  $\beta \in (-\pi/4, \pi/4]$ , the maximum of  $|j_{xy}|$  equals  $P$  and is achieved when the orientation angle  $\chi$  equals  $\pi/4$ .

## Appendix C: Parametrizations of qubits and polarization states

In this Appendix, we report for completeness some mathematical details on the parametrization of qubits and polarization states viewed as points on the Bloch sphere and the Poincaré sphere, respectively. These details help comprehending the schematic depictions in Fig. 1.

In terms of the computational basis vectors  $|0\rangle$  and  $|1\rangle$ , a normalized qubit is a point on the Bloch sphere that can be parametrized as

$$|\psi(\theta, \varphi)\rangle \stackrel{\text{def}}{=} \cos\left(\frac{\theta}{2}\right) |0\rangle + e^{i\varphi} \sin\left(\frac{\theta}{2}\right) |1\rangle, \quad (\text{C1})$$

with  $0 \leq \theta \leq \pi$  and  $0 \leq \varphi < 2\pi$ . The Bloch sphere metric is given by  $ds_{\text{Bloch}}^2 \stackrel{\text{def}}{=} d\hat{n}_B \cdot d\hat{n}_B = d\theta^2 + \sin^2(\theta) d\varphi^2$  with  $\hat{n}_B \stackrel{\text{def}}{=} \langle \psi(\theta, \varphi) | \vec{\sigma} | \psi(\theta, \varphi) \rangle = (\sin\theta \cos\varphi, \sin\theta \sin\varphi, \cos\theta)$  and  $\vec{\sigma} \stackrel{\text{def}}{=} (\sigma_x, \sigma_y, \sigma_z)$  being the usual vector of Pauli matrices.

In terms of the orthonormal circular basis states  $\hat{e}_{\text{RC}}$  (right circular) and  $\hat{e}_{\text{LC}}$  (left circular), the general equation of a normalized state of polarization  $\hat{e}(\beta, \chi)$  viewed as a point on the Poincaré sphere is given by

$$\hat{e}(\beta, \chi) \stackrel{\text{def}}{=} \frac{\cos(\beta) + \sin(\beta)}{\sqrt{2}} \hat{e}_{\text{RC}} + e^{i2\chi} \frac{\cos(\beta) - \sin(\beta)}{\sqrt{2}} \hat{e}_{\text{LC}}, \quad (\text{C2})$$

with  $-\pi/4 < \beta \leq \pi/4$  and  $0 \leq \chi < \pi$ . The Poincaré metric is given by  $ds_{\text{Poincaré}}^2 \stackrel{\text{def}}{=} d\hat{n}_P \cdot d\hat{n}_P = 4 [d\beta^2 + \cos^2(2\beta) d\chi^2]$  where  $\hat{n}_P \stackrel{\text{def}}{=} \langle \hat{e}(\beta, \chi), \vec{\sigma} \hat{e}(\beta, \chi) \rangle_{\mathbb{C}} = (\cos(2\beta) \cos(2\chi), \cos(2\beta) \sin(2\chi), \sin(2\beta))$ , with  $\langle \cdot, \cdot \rangle_{\mathbb{C}}$  denoting the usual complex inner product. From Eq. (C2), note that points on the poles specify circularly polarized light,  $\hat{e}_{\text{RC}} \stackrel{\text{def}}{=} \hat{e}(\pi/4, 0)$  and  $\hat{e}_{\text{LC}} \stackrel{\text{def}}{=} \hat{e}(-\pi/4, 0)$ . Furthermore, points on the equator correspond to linearly polarized light,  $\hat{e}_{\text{VL}} \stackrel{\text{def}}{=} \hat{e}(0, \pi/2)$  (vertical linear) and  $\hat{e}_{\text{HL}} \stackrel{\text{def}}{=} \hat{e}(0, 0)$  (horizontal linear). Ignoring an overall phase, we remark that  $\hat{e}_{\text{RC}} \stackrel{\text{def}}{=} (\hat{e}_{\text{HL}} - i\hat{e}_{\text{VL}})/\sqrt{2}$  and  $\hat{e}_{\text{LC}} \stackrel{\text{def}}{=} (\hat{e}_{\text{HL}} + i\hat{e}_{\text{VL}})/\sqrt{2}$ . Finally, the remaining points on the Poincaré sphere represent other elliptical polarization states.

## Appendix D: Interference effects in propagation of light, quantum searching, and optimal-speed quantum evolutions

In this Appendix, we present some comments on the role played by interference effects in light propagation, quantum searching, and optimal-speed quantum evolutions. These remarks integrate those presented in Section V.

In the study of propagation of light, coherent sources are required for producing interference patterns. In particular, interference of light beams appear in the calculation of the total intensity of the resultant beam obtained in terms of a superposition of two coherent beams. In this context, the objective is to obtain propagation of light with maximal degree of coherence. Maximization of the absolute value of the complex degree of coherence, interpreted as a measure of the degree of correlation of the electric vibrations of the wave, yield more visible interference patterns. Indeed, the degree of coherence establishes in a formal manner how distinctly visible is the interference pattern [78]. We note that to have a nonzero degree of coherence, the coherency matrix has to have nonvanishing off-diagonal terms [9, 25]. This observation becomes especially interesting when we recall that quantum computation derives its power from entanglement and quantum interference. In particular, the degree of interference in a  $N$ -qubit register is specified by the coherences, that is, the off-diagonal elements  $\rho_{lm}$  with  $l \neq m$  of the density operator in the computation basis. Therefore, the role played by coherences in quantifying the degree of quantum interference viewed as a source of power for quantum computing can be grasped in a straightforward manner [52]. These considerations lead us to the following question: Where does the phenomenon of quantum interference manifest itself in the quantum computational tasks considered in our paper?

In Grover's digital quantum search algorithm [31], the interference of quantum probability amplitudes appears in the calculation of the transition probability from the (known) source state to the (unknown) target state. Indeed, in quantum searching, the goal is to achieve unit transition probability (defined as the modulus squared of the quantum overlap between the target state and the source state acted upon by a number of iterations of Grover's operator) with the smallest number of iterations of Grover's operator. More specifically, quantum searching can be explained as inducing a desired relative phase between two eigenvectors of Grover's operator to yield constructive interference on the target state (that is, use quantum interference to nudge up the searched state) and destructive interference on the remaining states [48, 49]. In the Farhi-Gutmann analog quantum search evolution viewed as the continuous-time version of Grover's search scheme [46], the interference of quantum probability amplitudes emerges in the computation of the transition probability from the (known) source state to the (unknown) target state. The goal there is to achieve unit transition probability in the shortest amount of time. The Farhi-Gutmann search Hamiltonian specifies the dynamical process of quantum interference which, in turn, allows one to evolve from the source state to the target state in the smallest possible time by modifying the explored intermediate superpositions of quantum states in a suitably prescribed manner so that time optimality [54, 79] is achieved. Finally, in the optimal-speed quantum Hamiltonian evolutions [18, 19], interference of quantum probability amplitudes can be identified in the maximization of the energy uncertainty (that is, the dispersion of the Hamiltonian operator). This maximization is required in order to evolve from a (known) source state to a (known) target state with optimal-speed (that is, the maximum energy uncertainty and the smallest travel time). The optimal-speed time-independent Hamiltonian specifies, via its eigenvector decomposition, the process of quantum interference. The latter, in turn, allows us to transition from the source to the target states in the shortest possible time by navigating through a path of quantum states while preserving maximal energy uncertainty. Interestingly, we pointed out the correspondence between intensity of light and energy of the quantum system in the constraint equations that appear in Table II.